

Gravitons and Dark Matter in Universal Extra Dimensions

Nausheen R. Shah^{a,c} and Carlos E.M. Wagner^{a,b,c}

*Enrico Fermi Institute^a and Kavli Institute for Cosmological Physics^b,
University of Chicago, Chicago, IL 60637, USA*

^c*HEP Division, Argonne National Laboratory, 9700 Cass Ave., Argonne, IL 60439, USA*

August 28, 2018

Abstract

Models of Universal Extra Dimensions (UED) at the TeV scale lead to the presence of Kaluza Klein (KK) excitations of the ordinary fermions and bosons of the Standard Model that may be observed at hadron and lepton colliders. A conserved discrete symmetry, KK-parity, ensures the stability of the lightest KK particle (LKP), which, if neutral, becomes a good dark matter particle. It has been recently shown that for a certain range of masses of the LKP a relic density consistent with the experimentally observed one may be obtained. These works, however, ignore the impact of KK graviton production at early times. Whether the G^1 is the LKP or not, the G^n tower thus produced can decay to the LKP, and depending on the reheating temperature, may lead to a modification of the relic density. In this article, we show that this effect may lead to a relevant modification of the range of KK masses consistent with the observed relic density. Additionally, if evidence for UED is observed experimentally, we find a stringent upper limit on the reheating temperature depending on the mass of the LKP observed.

1 Introduction

Theoretical models constructed to understand physics beyond the standard model (SM) (most notably string theory) frequently imply the existence of extra dimensions. It has been a particular challenge in phenomenology to understand how these extra dimensions would be realized and manifested in our observable $3 + 1$ dimensional world. The number, shape and size of these dimensions, as well as the particles allowed to propagate in them give rise to several different models, all having different phenomenological implications.

We will be considering universal extra dimensions (UED) where the SM fields propagate in all the extra dimensions. For toroidal compactification, this would imply a tower of Kaluza-Klein (KK) particles for every SM particle, each carrying KK number. Momentum conservation in the extra dimensions implies KK number conservation. However, the requirement of obtaining the proper SM chiral modes at low energies leads to constraints on the possible compactification geometries. An example for $D = 5$ is the orbifold S^1/Z_2 where the Z_2 projects out half of the zero modes, leaving only SM fields. Additionally, this breaks translation invariance along the extra dimensions, so KK number is no longer conserved. A residual symmetry, KK-parity, is still present and it is sufficient to ensure the stability of the lightest KK particle (LKP). It also ensures that KK particles are always produced in pairs, allowing for good agreement between theory and experiment for small values of the compactification scale, of the order of a few hundred GeV [1, 2, 3].

The stability of the LKP allows for an interesting candidate for dark matter (DM) [4]. The LKP is expected to be weakly interacting and electrically neutral if it is to be considered a candidate for dark matter. The usual candidate is B^1 , the KK partner of the hypercharge gauge boson. For $m_{\text{KK}} \sim \mathcal{O}(1)$ TeV, B^1 gives excellent agreement with the observed relic density. There have been many further analyses of the relic density in UED, including a more proper treatment of coannihilation effects, and the impact of the inclusion of second KK level resonances [5, 6, 7, 8, 9, 10].

However, most of these studies ignore the gravitational sector. We shall mostly work within the context of one extra dimension. The gravitons couple extremely weakly and therefore are generally considered to be unimportant for collider studies. Cosmologically, however, they can have a significant effect¹, and they can also be a candidate for the LKP [12].

We are interested in investigating the inclusion of the graviton tower in the scenario with B^1 as the LKP. The gravitons do not evolve thermally, and have very long lifetimes, so if they are present, we expect them to decay to the LKP sometime after Big Bang Nucleosynthesis (BBN). The preservation of the light element abundances sets a bound on the amount of energy that can be released in a decay [13, 14, 15].

¹The radion can also be quite relevant [11]. We shall assume that the radion is inert during inflation and that it acquires a large mass, and therefore it does not have any impact on our analysis.

Secondly, since the gravitons decay ultimately into the LKP, we expect the relic density to increase. Therefore, the mass of the LKP consistent with the observed relic density is lowered. Additionally, if any of the gravitons decay after matter domination, we have to consider the effects of non-thermalized photons released in the decays on the spectrum of the diffuse photon flux (DPF) [16].

This article is organized as follows. In Section 2, we review the standard calculation for relic density. Section 3 reiterates the calculation for the density of gravitons presented in Ref. [12], emphasizing the points relevant for our analysis. In Section 4, we analyze the lifetimes for the decay of the graviton tower and study its implication on the diffuse photon spectrum. Section 5 goes over the constraints on the energy released in the decay of the KK gravitons to the LKP. In Section 6, we combine the above results with the standard relic density calculation. Our goal is to analyze the effect of the gravitons on the predicted mass of the LKP consistent with the known dark matter density. We will show that, in fact, almost any value of m_{KK} lower than the one obtained in the absence of gravitons would be allowed, provided the reheating temperature, T_R , is large enough. For the calculation of the relic density of B^1 , we ignore complicating factors such as coannihilation and second KK level resonance effects [5, 6, 7, 8, 10]. However, since these effects can be parameterized in the effective cross-section, we present the effect the graviton tower will have on the mass of the LKP without the gravitons, m_{WG} , and note that as m_{WG} increases, the contribution due to the graviton tower becomes large, and should be included in any precise calculation of m_{KK} . We also find that all the gravitons, except for G^1 , decay right after BBN. At these early times, the electromagnetic BBN constraints are very weak. However it has been shown that at small lifetimes, the hadronic constraints are very stringent [17, 18]. Therefore, including constraints from both hadronic and electromagnetic decays, requiring consistency with BBN light element predictions, we find a stringent limit on the mass difference between m_{G^1} and the LKP mass, m_{KK} . Since the G^1 is long-lived, we also derive another constraint on the mass difference such that the observed spectrum of the DPF is not destroyed. Comparing the two constraints, we find that there exists a region of parameter space where both constraints are satisfied and which gives mass differences of the same order of magnitude as that obtained by radiative loop corrections to m_{B^1} [19]. Additionally, we observe that if experimental evidence for UED is found, and the relic density induced by standard interactions of the KK modes is found to be lower than the one observed experimentally, the reheating temperature may be determined by assuming that the graviton KK modes provide the contribution necessary to achieve consistency between theory and experiment. Alternatively, including the possibility of other unobserved exotic particles contributing to the relic density, an upper bound on the reheating temperature is obtained.

2 Relic Calculation

Let us start by recalling the computation of the density of thermal relics. For any particle z , the evolution of the number density n_z is governed by the Boltzmann equation:

$$\frac{dn_z}{dt} + 3Hn_z = -\langle\sigma v\rangle (n_z^2 - n_{eq}^2) \quad (1)$$

$$H = \left(\frac{8\pi G_N \rho}{3}\right)^{1/2} \quad (2)$$

$$n_{eq} = g \left(\frac{mT}{2\pi}\right)^{3/2} e^{-m/T} \quad (3)$$

where $\langle\sigma v\rangle$ is the thermally averaged cross-section multiplied by the relative velocity, and Eq. (3) is valid in the non-relativistic approximation, with m and g being the mass and number of degrees of freedom associated with the particle z . The temperature at which the particle decouples from the thermal bath is denoted by T_F (*freeze-out temperature*) and roughly corresponds to when $\Gamma = n\langle\sigma v\rangle$ is of the same order as H .

Changing variables from n to $Y = n/s$ (we will drop the subscript z from now on), where the entropy density is given by $s = \frac{2\pi^2}{45}g_*T^3$, and using the fact that sR^3 remains constant, we obtain,

$$\dot{Y}s = -\langle\sigma v\rangle s^2(Y^2 - Y_{eq}^2). \quad (4)$$

Introducing the variable $x = \frac{m}{T}$, in the radiation dominated era:

$$H^2 = \frac{\pi^2 g_* T^4}{180 M_4^2}, \quad t = \frac{1}{2H} \quad \Rightarrow \quad \frac{dx}{dt} = H x. \quad (5)$$

Then, Eq. (4) may be rewritten as

$$\frac{dY}{dx} = -\frac{\langle\sigma v\rangle}{Hx} s (Y^2 - Y_{eq}^2). \quad (6)$$

We are interested in obtaining the relic density, or the equivalent Y_∞ , at late times. The solution of Eq. (6) enables the determination of the relic density and also the value of x_F as a function of Γ . The ratio of the mass to the freeze-out temperature, $x_F = m_{KK}/T_F$ is approximately given by

$$x_F = \ln \left(c(c+2)\sqrt{90\pi} \frac{g}{2\pi^3} \frac{m_{KK}M_4 \langle\sigma v\rangle}{g_*^{1/2} x_F^{1/2}} \right) \quad (7)$$

and can be solved iteratively, with $c \simeq 1/2$ and $M_4 = 1.7 \times 10^{15}$ TeV. As calculated in [4], for B^1 as the LKP, without including co-annihilation ², the non-relativistic approximation is:

$$\langle \sigma \nu \rangle = a + \frac{6b}{x} \quad (8)$$

$$a = \frac{4\pi\alpha_1^2(2Y_f + 3Y_B)}{9m_{\text{KK}}^2} = \frac{a'}{m_{\text{KK}}^2}, \quad (9)$$

$$b = -\frac{\pi\alpha_1^2(2Y_f + 3Y_B)}{18m_{\text{KK}}^2} = \frac{b'}{m_{\text{KK}}^2}, \quad (10)$$

where Y_f and Y_B denote a summation over the fourth power of the hypercharges of fermions and bosons produced in the annihilation of B^1 respectively. Moreover, ignoring the splitting between the different KK states of a given tower, one obtains, approximately

$$x_F = \ln \left[\frac{1.79 \times 10^{14} \text{ TeV}}{x_F^{1/2}} \frac{1}{m_{\text{KK}}} \left(a' + \frac{6b'}{x_F} \right) \right]. \quad (11)$$

In terms of this, Y_∞ is found to be:

$$\begin{aligned} Y_\infty^{-1} &= \frac{4\pi}{3} \sqrt{\frac{g_*}{5}} M_4 m_{\text{KK}} x_F^{-1} \left(a + \frac{3b}{x_F} \right) \\ &= \frac{3.05 \times 10^{16} \text{ TeV}}{x_F} \frac{1}{m_{\text{KK}}} \left(a' + \frac{3b'}{x_F} \right) \end{aligned} \quad (12)$$

where we have assumed masses of $\mathcal{O}(1)$ TeV, and used $g_* \simeq 92$ for $T_F \sim 50$ GeV and $s_0 = 2889.2 \text{ cm}^{-3}$. For more than one extra dimension this analysis is more complicated but a rough estimate may be obtained by assuming independent towers of KK modes for each extra dimension, d . The current relic energy density then is simply given by $\rho = m_{\text{KK}} s_0 d Y_\infty$. We will however restrict ourselves to one extra dimension in most of our numerical work.

As emphasized in the introduction, the above derivation for the density of B^1 ignores the contribution of the KK modes of the gravitons, which may become relevant for sufficiently large values of the reheating temperature T_R .

3 Density of KK Gravitons

After reheating, except for gravitons, all other particles are initially in equilibrium and follow the pattern described in the previous section. After dilution of their density due to inflation, the gravitons are produced mainly in collisions involving gauge

²The effects of including these corrections to the cross-section in our analysis are discussed in detail in Section 6.3.

bosons, either in the initial or the final state, with cross-sections proportional to α_i/M_4^2 , where α_i is the relevant gauge coupling. Since their density is so small, they are never in equilibrium and further we can ignore graviton annihilation processes to first order. Because the decay times for gravitons are of the order of $\tau \sim 10^7$ s, the gravitons produced in the early universe are still present when the LKP freezes out. As the universe cools down further, the gravitons start to decay. Including higher order mass corrections [19], we will have decays of the form:

$$G^n \rightarrow n \text{ LKP} + X \quad (13)$$

where X denotes SM particles. Here we are considering only KK number preserving decays since the KK number violating decays would only take place at the orbifold fixed points and so would only have a sizeable contribution in the case when the KK number preserving decays are suppressed due to phase space considerations. Hence, after decaying, the KK gravitons contribute to the LKP relic density and a proper computation of the dark matter density demands the addition of this effect to the relic density calculated in the previous section.

In order to obtain a quantitative estimate of this effect, we follow the derivation for the number density of gravitons presented in Ref. [12]. The number density of the KK gravitons at each level n is again determined by the Boltzmann equation:

$$\frac{dn_{G^n}}{dt} + 3Hn_{G^n} = C_{G^n}, \quad (14)$$

where C_{G^n} is the collision operator and can be parameterized as follows:

$$C_{G^n} = C\sigma[g_*(T)n_0]^2, \quad (15)$$

where

$$\sigma = \frac{\alpha_3}{4\pi M_4^2}. \quad (16)$$

Here α_3 is the strong coupling constant and C can be understood as the fraction of all possible collisions which will interact strongly to produce gravitons. The exact calculation of the total production cross section is quite complicated, but can be estimated by the method presented in Appendix A. The authors of Ref. [12] used an analogy with the calculation of gravitino abundances [20, 21], and estimated $C \sim \mathcal{O}(0.01)$. However the sample calculation of the cross-section for the production of relativistic gravitons presented in Appendix A leads us instead to expect $C \sim \mathcal{O}(1)$. For completeness we will consider a range of values, $0.01 \leq C \leq 1$, in our numerical work.

For UED theories, $g_*(T) = g_*^{KK}D_d(T)$, where g_*^{KK} is the effective number of degrees of freedom per KK level. $D_d(T)$ can be approximated by counting all modes with masses below T :

$$D_d(T) = \frac{1}{2^d} V_d \left[\frac{T}{m_{\text{KK}}} \right]^d \quad (17)$$

where

$$V_d = \frac{\pi^{d/2}}{\Gamma(1 + \frac{d}{2})} = 2, \pi, \frac{4}{3}\pi, \frac{1}{2}\pi^2, \dots \quad \text{for } d = 1, 2, 3, \dots, \quad (18)$$

is the d dimensional volume of a unit sphere, and the factor $1/2^d$ in Eq. (17) accounts for the restriction to non-negative n . Assuming entropy conservation, $S = sR^3 \propto g_*(T)T^3 R^3 \propto T^{3+d} R^3$:

$$\frac{1}{s} \frac{ds}{dt} = -3 \frac{1}{R} \frac{dR}{dt} = -3H, \quad \frac{dT}{dt} = -\frac{3}{3+d} HT. \quad (19)$$

As in the previous section, making the substitution $Y = n/s$ and with the help of Eq. (19) the Boltzmann equation becomes:

$$\frac{dY_{G^n}}{dT} = -\frac{3+d}{3} \frac{1}{HTs} C \sigma[g_*(T)n_0]^2. \quad (20)$$

Y_{G^n} changes until G^n production stops at temperatures $T \sim nm_{\text{KK}}$ and then remains constant until gravitons begin to decay. After BBN and before gravitons decay:

$$\begin{aligned} Y_{G^n} &= \frac{45\sqrt{5}\zeta^2(3)}{2\pi^8} \alpha_3 \frac{m_{\text{KK}}}{M_4} C \sqrt{g_*^{KK}} \frac{3+d}{2+d} \sqrt{\frac{V_d}{2^d}} \left[\left(\frac{T_R}{m_{\text{KK}}} \right)^{1+\frac{d}{2}} - n^{1+\frac{d}{2}} \right] \quad \text{for } n < \frac{T_R}{m_{\text{KK}}}; \\ &= 0 \quad \text{for } n > \frac{T_R}{m_{\text{KK}}}. \end{aligned} \quad (21)$$

To find the Y_G contribution to the LKP, assuming only KK number preserving decays,

$$\begin{aligned} Y_G &= \int_0^{T_R/m_{\text{KK}}} n Y_{G^n} d^n n \\ &= \frac{45\sqrt{5}\zeta^2(3)}{2\pi^8} \alpha_3 \frac{m_{\text{KK}}}{M_4} C \sqrt{g_*^{KK}} \frac{3+d}{(1+d)(4+3d)} \sqrt{\frac{V_d A_d^2}{2^{3d}}} \left[\frac{T_R}{m_{\text{KK}}} \right]^{2+\frac{3d}{2}} \\ &= \alpha(d) C \frac{m_{\text{KK}}}{\text{TeV}} \left[\frac{T_R}{m_{\text{KK}}} \right]^{2+\frac{3d}{2}} \end{aligned} \quad (22)$$

$$A_d = \frac{2\pi^{d/2}}{\Gamma(d/2)} = 2, 2\pi, \dots \quad \text{for } d = 1, 2, \dots, \quad (23)$$

where $\alpha_3 \sim 0.1$ and $g_*^{KK} \sim 200$.

4 Decay Lifetimes and Diffuse Photon Flux

The decay widths for the decay of the gravitons are calculated in Appendix B. As shown there, the decay of G^n for $n > 1$ is primarily into gauge bosons of KK number $n/2$ ($(n \pm 1)/2$ for n odd), assuming that all fermions are heavier. The lifetime for these is suppressed by powers of n , and is given by:

$$\begin{aligned}\tau(G^n) &= \frac{32\pi}{\sqrt{2}\cos^2\theta_W} \frac{M_4^2}{m_n^3} \sqrt{\frac{m_n}{\Delta_n}} \\ &\sim 1.76 \times 10^5 \text{ s} \left[\frac{\text{TeV}}{m_n} \right]^{5/2} \left[\frac{\text{TeV}}{\Delta_n} \right]^{1/2} \\ &\sim 5.56 \times 10^6 \text{ s} \frac{1}{n^3} \left[\frac{\text{TeV}}{m_{\text{KK}}} \right]^3\end{aligned}\tag{24}$$

where $\Delta_n \equiv m_{G^n} - 2m_{B^{\frac{n}{2}}} \ll m_{G^n}$ and in the last line we have approximated $\Delta_n \sim n\Delta_1 \equiv n(m_{G^1} - m_{B^1})$ with $\Delta_1 \sim 10^{-3}m_{\text{KK}}$, which is of the order of the mass corrections induced at one loop [19], and, as we will show below, is also of the order of the mass differences required to satisfy the phenomenological constraints coming from BBN and diffuse gamma ray constraints.

The only long-lived graviton is G^1 , with a lifetime given by:

$$\begin{aligned}\tau(G^1) &= \frac{3\pi}{\cos^2\theta_W} \frac{M_4^2}{\Delta_1^3} \\ &\sim 2.33 \times 10^4 \text{ s} \left[\frac{\text{TeV}}{\Delta_1} \right]^3, \\ &\sim 2.33 \times 10^{13} \text{ s} \left[\frac{\text{TeV}}{m_{\text{KK}}} \right]^3,\end{aligned}\tag{25}$$

where we have again assumed in the last line that $\Delta_1 \sim 10^{-3}m_{\text{KK}}$. The different dependence on the mass difference in Eq. (24) and (25) is due to the fact that one of the decay products for G^1 is massless.

The diffuse photon flux is only sensitive to photons released after matter domination [16, 22] since the late produced photons don't have time to thermalize. Therefore we just need to ensure that the energy released in the decay of the G^1 does not destroy the spectrum. The diffuse photon flux is given by [22]:

$$\frac{d\Phi}{dE_\gamma} \sim \frac{3c}{8\pi} \frac{N_{G^1}^{\text{in}}}{V_0 \epsilon_\gamma} \left[\frac{t_0}{\tau_{G^1}} \right] \left[\frac{E_\gamma}{\epsilon_\gamma} \right]^{1/2} e^{-\left[\left(\frac{E_\gamma}{\epsilon_\gamma} \right)^{3/2} \frac{t_0}{\tau_{G^1}} \right]} \Theta(\epsilon_\gamma - E_\gamma),\tag{26}$$

where ϵ_γ is initial energy released in the decay, E_γ is energy of photons observed now, t_0 and V_0 are the current time and volume of the universe, and $N_{G^1}^{\text{in}}$ is the total number of G^1 s initially. Using Y_{G^1} calculated in the previous section:

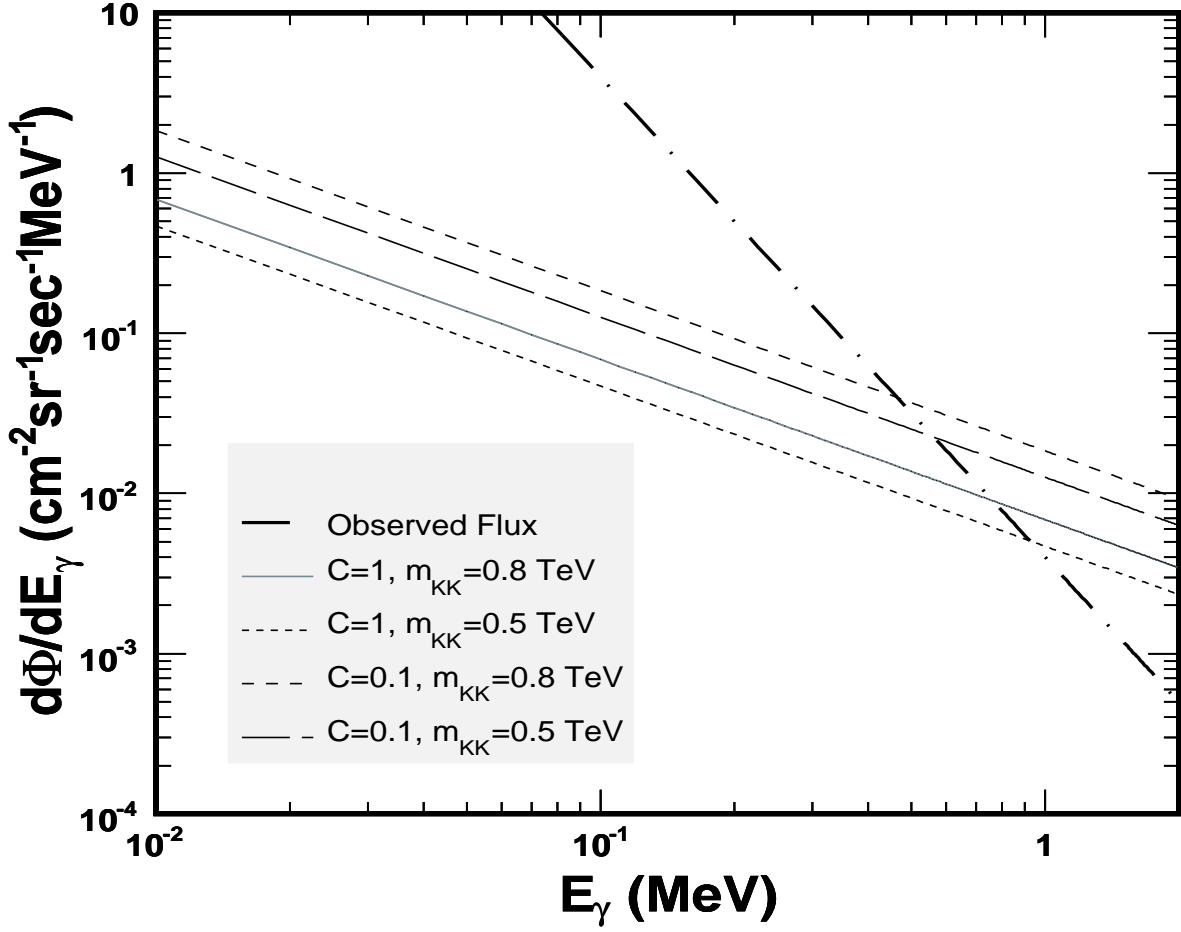


Figure 1: The observed Diffuse Photon Flux plotted in addition to the maximum flux from Eq. (29) for different values of C and m_{KK} , assuming T_R such that $\Omega_{B^1} = 0.23$.

$$\begin{aligned} \frac{d\Phi}{dE_\gamma} = & 1.63 \times 10^{-9} \text{sr}^{-1} \text{s}^{-1} \text{cm}^{-2} \text{MeV}^{-1} \left[\left(\frac{T_R}{m_{KK}} \right)^{3/2} - 1 \right] \\ & \left[\frac{\Delta_1}{\text{MeV}} \right]^{3/2} \left[\frac{m_{KK}}{\text{TeV}} \right] \left[\frac{E_\gamma}{\text{MeV}} \right]^{1/2} e^{- \left[\left(\frac{E_\gamma \Delta_1}{\text{MeV}^2} \right)^{3/2} 1.85 \times 10^{-5} \right]}. \end{aligned} \quad (27)$$

This has maximal value at:

$$E_\gamma^{max} = \epsilon_\gamma \left(\frac{\tau_{G^1}}{3t_0} \right)^{2/3} \simeq 0.687 \text{ MeV} \left[\frac{\text{GeV}}{\Delta_1} \right]. \quad (28)$$

Observe that, although ϵ_γ is proportional to Δ_1 , the inverse dependence of E_γ^{max} on Δ_1 comes from the energy redshift induced by the expansion of the Universe

($\tau_{G^1} \propto \Delta_1^{-3}$). This, in turn, leads to a maximum value for the flux,

$$\frac{d\Phi^{max}}{dE_\gamma} = 3.06 \times 10^{-5} \text{ sr}^{-1} \text{ s}^{-1} \text{ cm}^{-2} \text{ MeV}^{-1} \left[\left(\frac{T_R}{m_{KK}} \right)^{3/2} - 1 \right] \left[\frac{\Delta_1}{\text{GeV}} \right] \left[\frac{m_{KK}}{\text{TeV}} \right]. \quad (29)$$

If, for example, we assume a reheating temperature $T_R \sim 50 m_{KK}$, we obtain

$$\frac{d\Phi^{max}}{dE_\gamma} = 1.1 \times 10^{-2} \text{ sr}^{-1} \text{ s}^{-1} \text{ cm}^{-2} \text{ MeV}^{-1} \left[\frac{\Delta_1}{\text{GeV}} \right] \left[\frac{m_{KK}}{\text{TeV}} \right]. \quad (30)$$

This is two orders of magnitude less than was obtained in Ref. [22] for a similar mass range, and is marginally consistent with the observed diffuse photon flux [16]. The source of the difference is not computational, but based on the different assumptions made in both works. In Ref. [22], the NLKP was assumed to be B^1 and had a density comparable to the dark matter relic density, while in our framework we are concerned with the decay of the G^1 s, which have a density much smaller than that associated with the dark matter relic density.

In order to understand the constraints imposed by the photon flux on the G^1 decay, we can parameterize the experimentally observed flux in terms of E_γ as follows,

$$\frac{d\Phi}{dE_\gamma} \simeq 4 \times 10^{-3} \text{ sr}^{-1} \text{ s}^{-1} \text{ cm}^{-2} \text{ MeV}^{-1} \left[\frac{\text{MeV}}{E_\gamma} \right]^3. \quad (31)$$

This is plotted in Fig. 1. For comparison we have also plotted the maximum flux according to Eq. (29) for a range of values of C and m_{KK} , assuming a T_R such that $\Omega_{B^1} = 0.23$. The mass difference allowed by the diffuse photon flux can then be quantified by requiring that the maximum differential flux calculated from Eq. (29) is less than the observed flux Eq. (31). It should also be noted that here we assumed that all the photons produced in the decay of the gravitons did not thermalize and are available to distort the spectrum now. This is certainly an overestimate. The constraints on Δ_1 will be discussed in more detail in Section 6.6.

5 Energy Released in Decays

The electromagnetic showers produced by the decay of $G^n \rightarrow n \text{ LKP} + X$ can create and destroy light elements. As discussed in [13, 14, 15], this sets constraints on the lifetime τ of the unstable G^n as well as on ξ_γ , the energy released per background photon in the decay.

The dependence on τ can be understood by looking at the characteristic energy scales in the initially produced photon spectrum. The primary photon created in the decay interacts with the background and creates an EM cascade. The fastest interactions are pair production and inverse compton scattering. These processes rapidly redistribute the energy and the non-thermal photons reach a quasi-static

equilibrium (QSE). The zeroth order QSE photon spectrum depends inversely on the temperature of the background plasma. If we make the *uniform decay* approximation, i.e. all particles decay at $t = \tau$, this corresponds to a cut-off energy of $E_C = 103 \text{ MeV } (\tau/10^8 \text{ s})^{1/2}$ [15]. Therefore higher energy photo-erosion processes occur for longer lifetime values.

We can understand the ξ_γ dependance of photodestruction and secondary production in a similar way. In the limit of small ξ_γ , the decaying particle does not influence the light element abundances. Beyond this trivial case, we can again use the uniform decay approximation to gain some insights. As long as a reaction can take place (E_{TH} , the threshold energy for a reaction, $\lesssim E_C$), a typical shower photon has energy:

$$\langle E \rangle = 56 \text{ MeV } \left(\frac{E_{TH}}{10 \text{ MeV}} \right)^{1/2} \left(\frac{\tau}{10^8 \text{ s}} \right)^{1/4}. \quad (32)$$

Therefore, the number of such photons per decay is $N_\gamma \sim \delta m_{KK} / \langle E \rangle$, where δm_{KK} is the energy released in each decay. Thus, the non-thermal photon density is:

$$n_\gamma = N_\gamma n_{NLKP} = \frac{\xi_\gamma n_\gamma^{BG}}{\langle E \rangle} \quad (33)$$

These photons then further thermalize as well as cause photodestruction of particles to yield other species of particles. Therefore the dependence of the fractional change in the abundance of a particle is proportional to ξ_γ and inversely proportional to $\langle E \rangle$ and therefore to τ .

Detailed numerical work gives a complicated but weak constraint on ξ_γ for getting the correct light element abundances for small lifetimes. However after about $\tau > 10^7 \text{ s}$, the dependance on ξ_γ steadies out to $\xi < 10^{-15} \text{ TeV}$ [13, 14, 15]. Comparing Eq. (24) and (25), we see that the only long-lived graviton is the G^1 with $\tau(G^1) \sim 10^{13} \text{ s } \left[\frac{\text{TeV}}{m_{KK}} \right]^3$, much larger than 10^7 s . Hence, electromagnetic energy release bounds only constrain the decay of the G^1 to the LKP.

Similarly, hadrons produced in the decays can scatter off photons, electrons and, more importantly, background nuclei. Scattering off photons and electrons just causes them to lose energy, but the nuclei become more energetic and cause “hadronic showers”. Additionally if inelastic scattering occurs, the background nuclei get dissociated and the light element abundances are changed. Due to the multitude of possible interactions, these are a lot more complicated to analyze than the purely electromagnetic case. Previously it had always been assumed that since the branching ratio into hadrons is small, the effect would also be negligible. However detailed numerical work [17, 18] shows that in fact at early times, the constraints due to hadronic processes are much stronger than those due to electromagnetic processes.

As can be seen from Eq. (24) the lifetime of the G^n s are suppressed by powers of n : $\tau(G^n) \sim 10^6 \text{ s } \frac{1}{n^3} \left[\frac{\text{TeV}}{m_{KK}} \right]^3$. Therefore all the G^n s except for G^1 decay right

after BBN. The bounds at these relatively early decay times depend strongly on the branching ratio of the decay of the gravitons into hadrons. If all the visible energy released is in the form of hadrons, the bounds are quite severe: $\xi_H < 10^{-15}$ TeV. If most of the decay is into leptons, then the bounds on ξ_H may be significantly weaker. A preferential decay into leptons could happen if, for any given tower, the KK leptons are very close in mass to the KK hypercharge gauge bosons, while the KK quarks are heavier (see Appendix B for calculation of the graviton decay widths into fermions). This would be the result one would obtain if including only the radiative corrections to the KK particle masses computed in Ref. [19]. Since this is very model dependent, we will again use the most constrained case of $\xi_H < 10^{-15}$ TeV.

Hence, both for early and late time decays we will use a conservative bound for the energy released per background photon, $\xi_B < 10^{-15}$ TeV, in our numerical work. Observe that while strong violations of this bound will certainly induce strong effects on the light element abundances, and therefore are ruled out, small violations of this bound are still possible due to the fact that we used very conservative limits on the energy released.

One loop effects introduce corrections of two forms, constant (independent of n) and proportional to n (bulk and boundary correction terms)[19]. Therefore, the mass of a particle at KK level n can be written as:

$$m_n = \frac{n}{R} (1 + \delta) + \delta' \quad (34)$$

where the corrections δ and δ' for each particle type is the same at each level. The graviton KK modes, of course, do not receive corrections of this kind at the one loop level, and we shall assume, for simplicity, that their masses remain unperturbed: $m_{G^n} = n/R$.

To analyze the effects of the decays, we are going to treat the two cases ($\delta, \delta' = 0$) separately. Note that this is only for ease of understanding. In fact, the true effect would just be the sum of the two terms. In the decay $G^n \rightarrow nB^1 + X$ assuming that X is massless to first order, $m_{G^1} \sim m_{B^1}$, and small momenta, the energy released in each decay is given by:

$$E_X^n = \frac{m_{G^n}^2 - n^2 m_{B^1}^2}{2m_{G^n}} \sim \begin{cases} nm_{\text{KK}}\delta & \text{for } \delta' = 0 \\ \delta' & \text{for } \delta = 0. \end{cases} \quad (35)$$

For this energy release to be consistent with the light element abundances [13, 14, 15] we need to have:

$$\xi = \int_0^{T_R/m_{\text{KK}}} B_{\text{EM/Had}} \frac{n_{G^n}}{n_\gamma} E_X^n d^d n < \xi_B = 10^{-15} \text{ TeV} \quad (36)$$

here $n_{G^n} = s_0 Y_{G^n}$ as given in Eq. (21), and $B_{\text{EM/Had}}$ is the electromagnetic/hadronic branching ratio. This fraction depends on whether the LKP is a lepton or a gauge

boson and the mass splittings at each KK level [23]. Throughout this article we choose $B_{\text{EM/Had}} = 1$ as the most stringent constraint possible.

6 Determination of the Lightest KK Particle Mass

In this section, we will discuss the determination of the lightest KK particle mass consistent with the observed dark matter relic density. Since the energy density of LKP is determined, in part, by the primordial graviton KK density, the lightest LKP mass m_{KK} will depend on the reheating temperature and the parameter C governing graviton production at early times.

6.1 T_R Reheating Temperature

Including the decay of the gravitons in the density for B^1 , we have:

$$Y_{B^1} = dY_\infty + Y_G \quad (37)$$

$$n_{B^1} = s_0 Y_{B^1} \quad (38)$$

$$\Omega_{B^1} = \frac{m_{B^1} n_{B^1}}{\rho_c} \quad (39)$$

where $\rho_c = 5.3 \times 10^{-9} \text{ TeV/cm}^3$, and Y_∞ is the abundance of the LKP without the inclusion of the gravitons, Eq. (12), and Y_G is the abundance of the gravitons, Eq. (22). We have not included either coannihilation or second KK resonance effects in the calculation of Y_∞ .

Requiring that $\Omega_{B^1} \simeq 0.23$, we get :

$$T_R \simeq m_{\text{KK}} \left[\frac{\Omega_{B^1} \rho_c - s_0 m_{\text{KK}} d Y_\infty}{\alpha(d) C s_0 m_{\text{KK}}^2} \right]^{\frac{2}{4+3d}} \quad (40)$$

In principle, the above expression shows that the relic density constraint can be satisfied for any value of the lightest KK mode mass, m_{KK} , provided the value of T_R is adjusted according to Eq. (40). In practice, Fig. 2 shows that in order to get a consistent dark matter density for low values of m_{KK} , one would need large values of the ratio of the reheating temperature to m_{KK} , but as is discussed in the next section, these are disfavored due to strong coupling constraints. Similar results are presented in Fig. 3 for the case of $D = 6$.

The mass of the LKP that would be obtained without the graviton tower contribution, m_{WG} , is shown in the figure as the point where the bound on T_R becomes very strong, $m_{\text{KK}} \sim 0.92 \text{ TeV}$ for $D = 5$ and $m_{\text{KK}} \sim 0.65 \text{ TeV}$ for $D = 6$, since in this case the reheating temperature must become smaller than the lightest KK mass so that the relic density is not effected in any significant way by the gravitons.

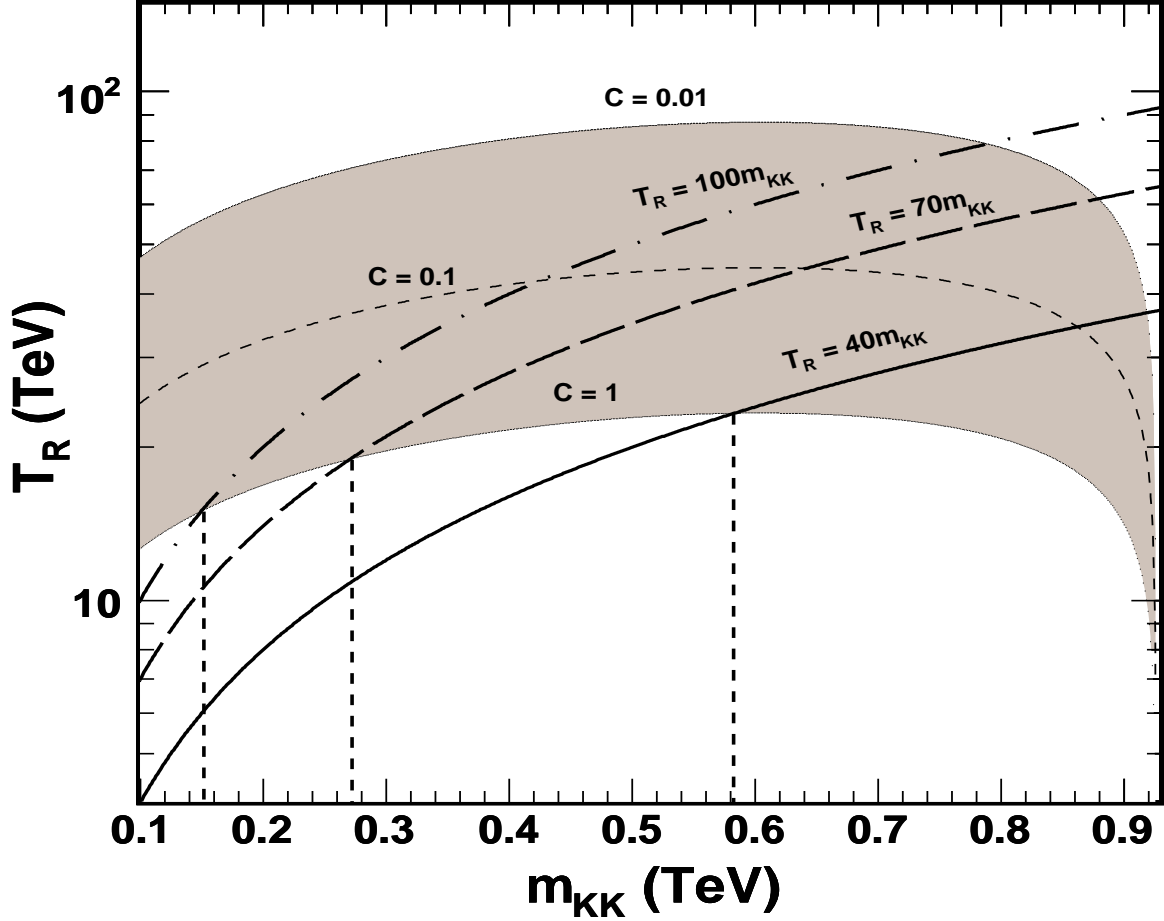


Figure 2: Values of the reheating temperature T_R obtained by demanding a proper dark matter density, $\Omega_{B^1} = \Omega_{\text{DM}} \simeq 0.23$, for different values of the graviton production parameter $C = 1, 0.1, 0.01$, and assuming $D = 5$. Also shown are lines of constant ratios of the reheating temperature to the lightest KK mass, $T_R = 40 m_{\text{KK}}$, $70 m_{\text{KK}}$ and $100 m_{\text{KK}}$.

It is important to stress that for $D = 5$, values of the KK masses smaller than about 500 GeV, are also restricted in the minimal UED case by precision electroweak constraints [2, 3, 24, 25]. Somewhat lower masses may be obtained for large values of the Higgs mass. However even then, within this minimal framework, values of m_{KK} smaller than 350 GeV are strongly disfavored. From Fig. 2 we see that for $D = 5$, $C \sim 1$ and values of the reheating temperature $T_R \leq 40 m_{\text{KK}}$ (consistent with the strong coupling bounds discussed in the next section), a consistent relic density may be obtained for any value of m_{KK} larger than 580 GeV. This range of values of the LKP mass are also consistent with precision electroweak constraints. Even for $C \sim 0.1$ and for the same range of values for the reheating temperature there could be modifications of m_{KK} up to ten percent of the value obtained without

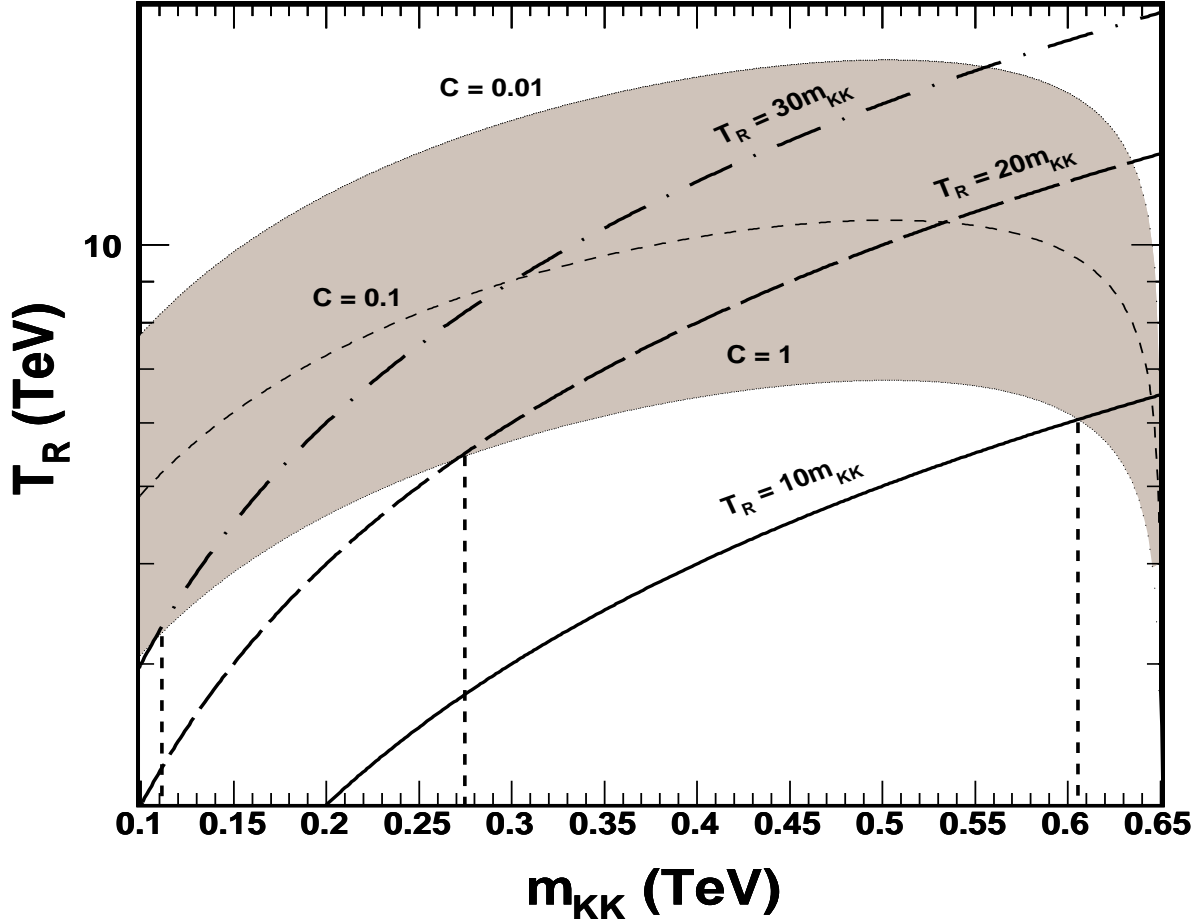


Figure 3: Values of the reheating temperature T_R consistent with the requirement $\Omega_{B^1} = \Omega_{DM} = 0.23$, for $C = 1, 0.1, 0.01$, and assuming $D = 6$. Also shown in the Figure are curves of constant ratio of the reheating temperature to the lightest KK mode, $T_R = 10 m_{KK}$, $20 m_{KK}$ and $30 m_{KK}$.

the inclusion of gravitons. Larger (smaller) modifications are possible for larger (smaller) values of T_R .

As shown in Fig. 3, for $D = 6$ one could obtain larger effects for smaller values of the ratio of T_R/m_{KK} . However, as will be shown in the next section, the bounds obtained from the requirement of perturbative consistency of the theory become much more stringent in this case. Therefore, large departures from the m_{KK} values obtained in the absence of gravitons seem to be disfavored for $D = 6$ within this minimal framework.

6.2 Constraints on the Reheating Temperature

Large values of the reheating temperature compared to m_{KK} immediately raise the question of the ultraviolet cut-off for our effective 4D theory. In Ref. [2], the authors assumed the limit on the KK masses to be the order of $\sim 40 m_{\text{KK}}$, based on the quantum corrections to the strong gauge coupling. More stringent bounds have been evaluated in [26, 27, 28]. Here we show that, if one computes the running of the zero mode hypercharge gauge coupling, and require it to remain weak in the ultraviolet regime, one obtains a bound similar to the one obtained in Ref. [2].

Let us then analyze the running of the zero mode gauge couplings for one extra dimension:

$$g_j^{-2}(\mu) = g_j^{-2}(m_z) - \frac{b_j}{8\pi^2} \ln \frac{\mu}{m_z} - \frac{\tilde{b}_j}{8\pi^2} (N_{\text{KK}} \ln[N_{\text{KK}}] - \ln[N_{\text{KK}}!]) \quad (41)$$

where

$$\begin{aligned} \tilde{b}_j &= \left(\frac{81}{10}, \frac{(-44 + 48 + 1 + 2d)}{6}, \frac{(-22 + 16 + d)}{2} \right), \text{ each KK level} \\ b_j &= \left(\frac{41}{10}, -\frac{19}{6}, -7 \right) \text{ SM} \end{aligned} \quad (42)$$

For $D = 5$, the most dangerous one for the KK scenario was the U(1) case and we found that g_1 develops a Landau pole at scales $\mu > 46 m_{\text{KK}}$ [29, 30, 31]. Our conclusion is then that above energy scales of about $40 m_{\text{KK}}$ our effective theory breaks down. Similarly, for $D = 6$, a Landau pole would develop at scales larger than about $10 m_{\text{KK}}$. However, these bounds may be avoided by assuming that this theory is just the low energy manifestation of a theory with more degrees of freedom and based on a higher, asymptotically free, gauge group. This would not only prevent α_1 from developing a Landau pole, but additionally it would increase the value of C . We have conservatively kept values up to $T_R \sim 100 m_{\text{KK}}$ for $D = 5$ and $T_R \sim 30 m_{\text{KK}}$ for $D = 6$.

The impact of these bounds on the possible values of the lightest KK mass are displayed in Figs. 2 and 3. As we mentioned before, we see that if we restrict ourselves to the bounds implied by perturbative consistency, the mass of the LKP can be as low as $m_{\text{KK}} \sim 0.6 \text{ TeV}$ for both $D = 5$ and $D = 6$, but lower values, as low as those implied by consistency with precision electroweak measurements, would be only obtained by the possible relaxation of these bounds by new physics. On the other hand, if the most stringent bounds obtained in [26, 27, 28] were imposed, very small modifications to the mass of the LKP would be obtained.

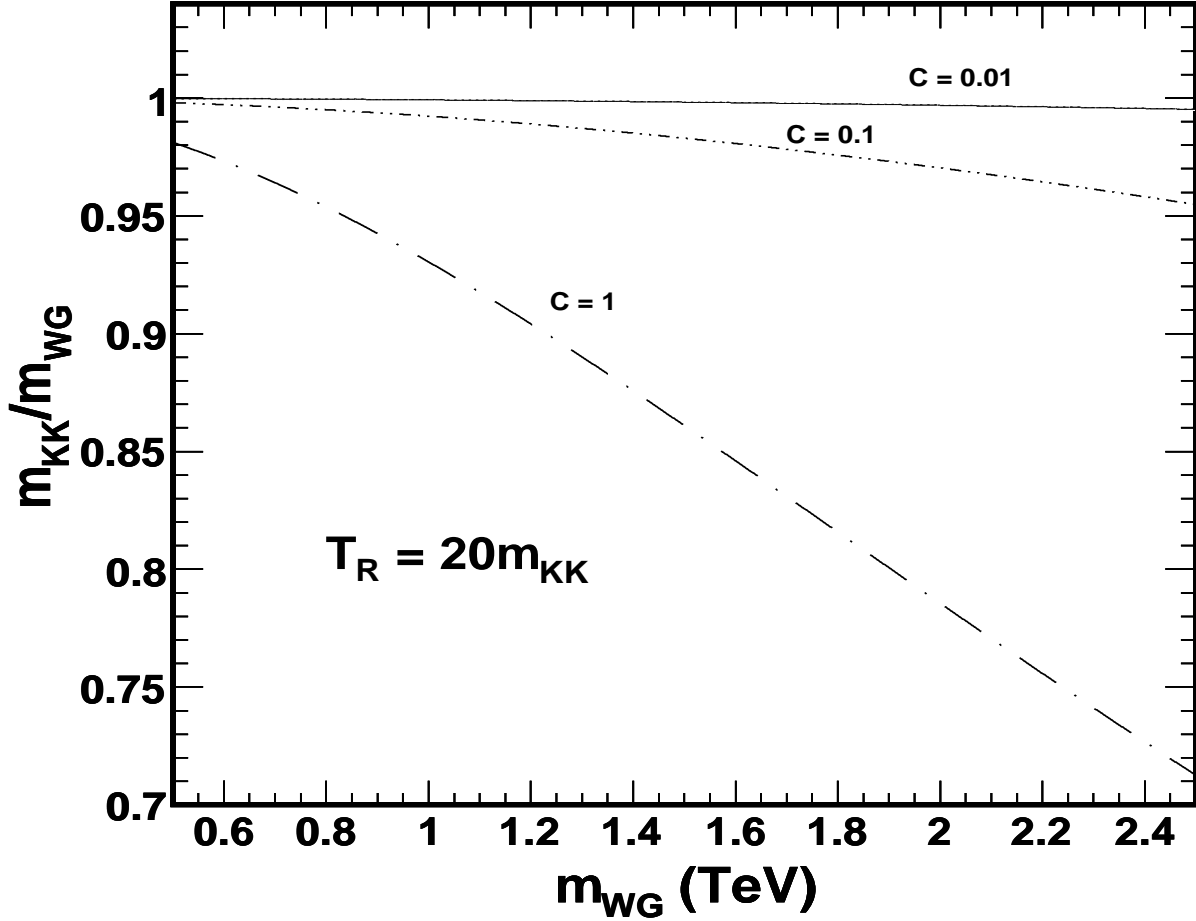


Figure 4: Values of the ratio of the LKP mass consistent with $\Omega_{DM} = 0.23$ to the one obtained in the absence of gravitons, m_{WG} , for $T_R = 20 m_{KK}$, $D = 5$ and for $C = 0.01, 0.1$ and 1 .

6.3 Additional Contributions to the Annihilation Cross Section

Until now, we have only considered the effects induced by the annihilation of B^1 s on the total relic density. However, several effects can change the density of the B^1 s. For example, if we assume that the mass difference between the LKP and the NLKP is less than about 10%, the NLKP is still thermally accessible to the LKP, and the effective cross-section, including coannihilations must be used in Eq. (1). Also, possible resonant effects induced by the second KK-level modes must be included [5, 6, 7, 8, 10]. Note that even though including these effects changes the mass of the LKP consistent with the dark matter density without the inclusion of the gravitons, m_{WG} , and will certainly change any numerical results we obtain, the qualitative picture we have presented here will remain unchanged.

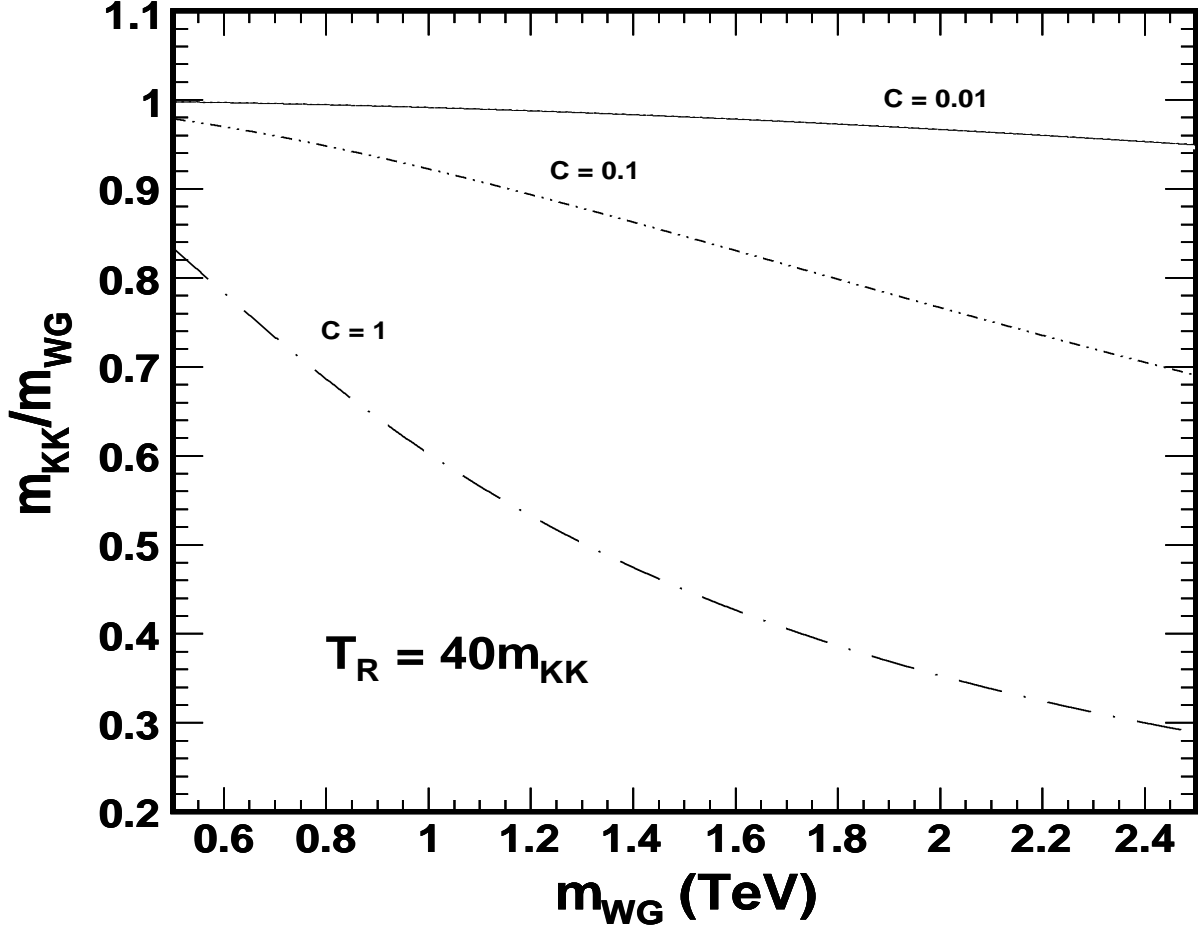


Figure 5: Same as Fig. 4, but for $T_R = 40 m_{KK}$.

The corrections to the cross-section can be quantified by considering a' and b' in Eq. (12) to encode all the information about the processes that affect Y_∞ . Due to the weak, logarithmic dependence of x_F on m_{KK} and the interaction cross section, we can approximately parameterize Y_∞ as being proportional to m_{KK} ,

$$Y_\infty = y \left(\frac{m_{KK}}{\text{TeV}} \right). \quad (43)$$

Then y , such that m_{WG} (including coannihilation, second KK resonances etc., but without the graviton tower) is consistent with the experimentally observed dark matter density, Ω_{DM} , is given by:

$$y = \frac{\rho_c \Omega_{DM}}{s_0 d m_{WG}^2}. \quad (44)$$

We can now replace Y_∞ using Eq. (43) and (44) in Eq. (37). Using this, we get

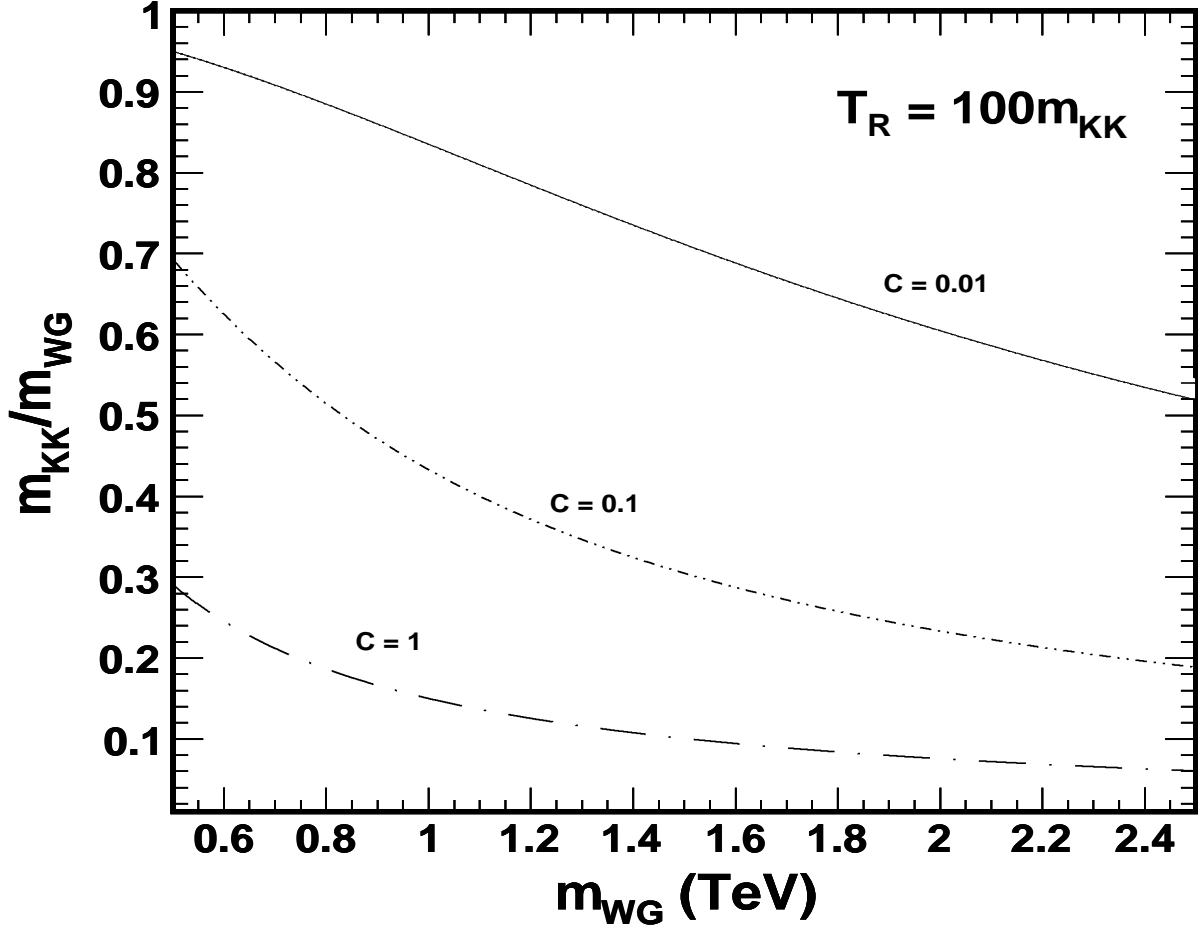


Figure 6: Same as Fig. 4, but for $T_R = 100 m_{KK}$.

the change in m_{WG} necessary to reproduce the observed dark matter density for a given reheating temperature T_R :

$$\frac{m_{KK}}{m_{WG}} = \left(\frac{\Omega_{DM} \rho_c}{\Omega_{DM} \rho_c + \alpha(d) C s_0 m_{WG}^2 \left[\frac{T_R}{m_{KK}} \right]^{\frac{4+3d}{2}}} \right)^{1/2} \quad (45)$$

This is plotted in Fig. 4, 5 and 6 for $T_R = 20 m_{KK}$, $40 m_{KK}$ and $100 m_{KK}$ and a range of m_{WG} predicted in Refs. [5, 6, 7, 8, 10]. We see that even for $T_R = 20 m_{KK}$ with $C = 1$, the mass consistent with the observed relic density undergoes a relevant modification due to the inclusion of the gravitons. This effect becomes increasingly important with increasing m_{WG} . Therefore, depending on the reheating temperature, any precise calculation of m_{KK} must include the contribution from the graviton tower to be accurate.

It is interesting to observe that for $T_R \simeq 100 m_{\text{KK}}$ and $C \simeq 1$, the necessary values of m_{KK} are below the bounds imposed by precision electroweak constraints. Conversely, this shows that for this value of C and for values of the KK masses consistent with precision electroweak constraints, such large values of the reheating temperature will lead to an excess of dark matter density and are therefore disfavored. On the contrary, for values of $T_R \lesssim 40 m_{\text{KK}}$, the obtained values of m_{KK} are in good agreement with the scale set by precision electroweak data. This shows an interesting correlation between the dark matter density bounds and those coming from requiring the perturbative consistency of the theory up to scales of the order of T_R .

6.4 Constraints on the G^1 – B^1 Mass Difference for $\delta' = 0$

In the discussion above, we have ignored the bounds on the energy released in the graviton decays. As we have stated in section 4, the amount of energy released will depend on the type of mass correction the graviton and B^1 receive (see Eq. (35) and Eq. (36)). For the case of $\delta' = 0$, the energy released per background photon is given by

$$\xi = \frac{B_{\text{EM/Had}}}{n_\gamma} \delta m_{\text{KK}} s_0 Y_G < \xi_B = 10^{-15} \text{ TeV}. \quad (46)$$

Assuming, as stated before, that there are no corrections to the KK graviton masses m_{G^n} , then $m_{G^n} = n m_{G^1}$. In addition we can identify m_{KK} with m_{B^1} . The corrections to $m_{B^1} = m_{G^1}(1 - \delta)$ are then equivalent to corrections to $m_{G^n} = n m_{B^1}(1 + \delta)$ for small δ .

If we now assume that the reheating temperature is such that one reproduces the correct dark matter relic density, $\Omega_{B^1} = 0.23$, as obtained in the previous section, then we get a constraint on the mass difference between G^1 and B^1 :

$$\delta m_{\text{KK}} < \frac{n_\gamma \xi_B}{B_{\text{EM/Had}}(\rho_c \Omega_{B^1} - m_{\text{KK}} s_0 d Y_\infty)}. \quad (47)$$

This is plotted in Fig. 7 for $D = 5$. This constraint is independent of C . The mass difference between B^1 and G^1 is very tightly constrained to be less than a GeV for most of the mass range considered. As m_{KK} approaches the value of the mass consistent with a proper dark matter relic density in the absence of gravitons, the bounds become very weak. This is due to the fact that in this case, as mentioned before, T_R may be of the order of (or smaller than) m_{KK} , and hence very few gravitons would be produced, implying that the mass difference can be large without inducing any dramatic effects.

For most of the parameter space, we have derived here a very stringent constraint on the mass difference. Therefore, we need to consider whether such small mass differences would require too much fine tuning to be considered natural. As is

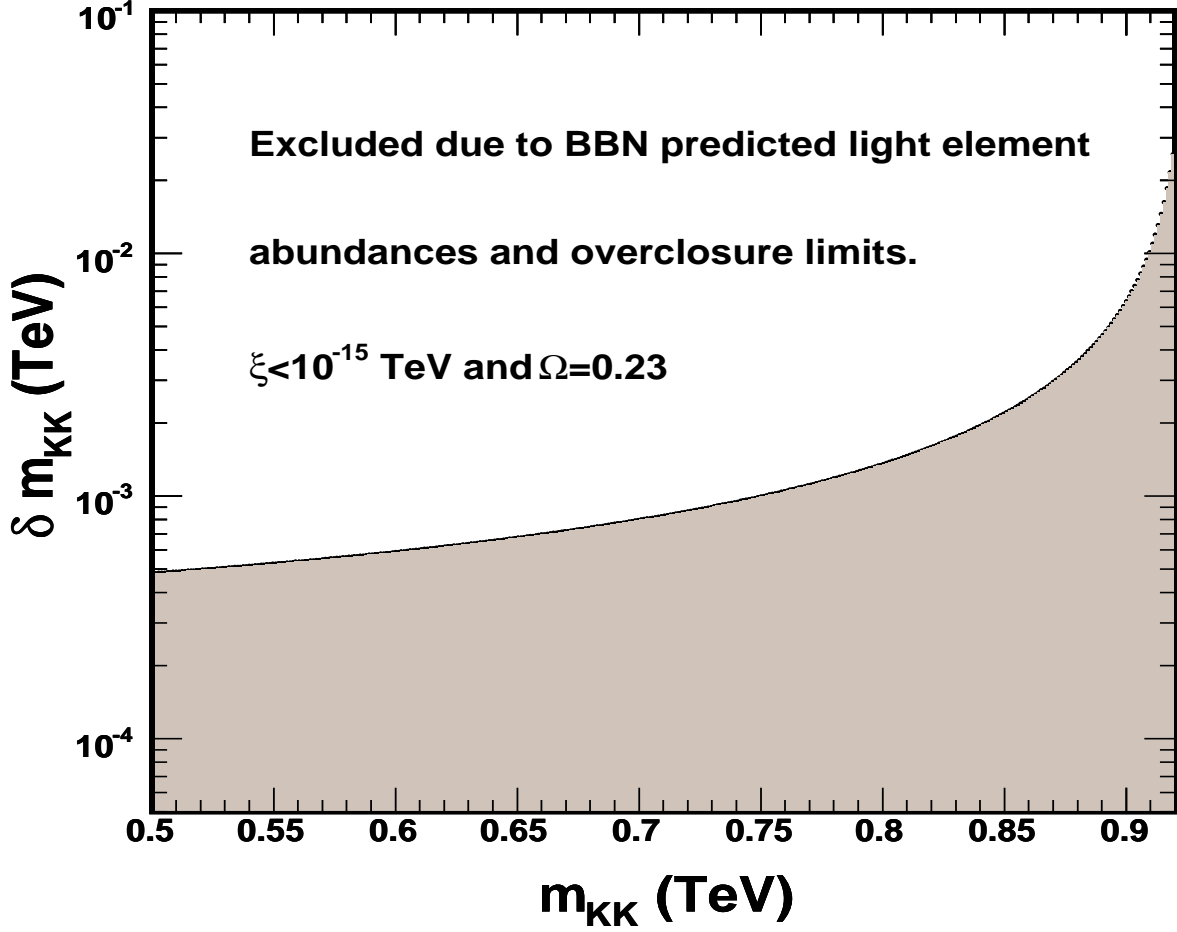


Figure 7: Values of the allowed mass difference between G^1 and the LKP, δm_{KK} , for $\delta' = 0$, assuming $\Omega_{DM} = 0.23$ and $\xi < 10^{-15}$ TeV for $D = 5$. We have ignored possible coannihilation and second KK level effects.

discussed in Section 6.7, we find that in fact the mass differences obtained here are the order of magnitude of the one loop corrections induced to the B^1 mass.

6.5 $\delta = 0$

Here we depart from the previous assumption and assume that all graviton KK modes receive a constant, positive mass correction with respect to nm_{KK} . The energy released for this kind of mass correction tends to be much smaller than in the case of $\delta \neq 0$ analyzed above (see Eq. (46)), and is given by:

$$\xi = \frac{B_{EM/Had}}{n_\gamma} \delta' s_0 Y'_G < \xi_B = 10^{-15} \text{ TeV} \quad (48)$$

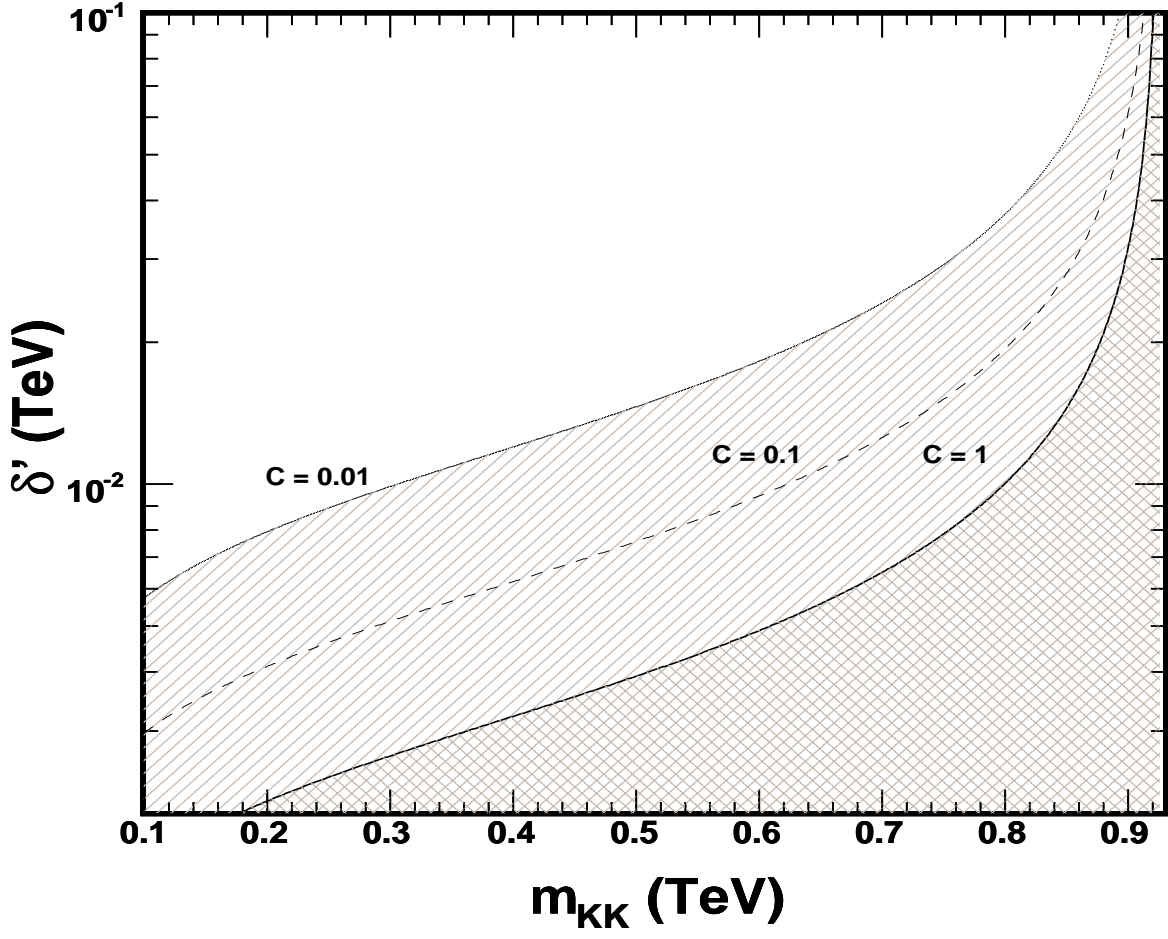


Figure 8: Values of δ' if $\Omega_{\text{DM}} = 0.23$ and $\xi < 10^{-15}$ TeV for $D = 5$, $C = 1, 0.1$ and 0.01 . We have ignored possible coannihilation and second KK level effects.

$$\begin{aligned}
Y'_G &= \int Y_{G^n} d^n n \\
&= \frac{45\sqrt{5}}{2\pi^8} \zeta^2(3) \alpha_3 \frac{m_{\text{KK}}}{M_4} C \sqrt{g_*} \sqrt{\frac{V_d A_d^2}{2^{3d}}} \frac{3+d}{d(2+3d)} \left[\frac{T_R}{m_{\text{KK}}} \right]^{1+\frac{3d}{2}} \\
&= \beta(d) C \frac{m_{\text{KK}}}{\text{TeV}} \left[\frac{T_R}{m_{\text{KK}}} \right]^{1+\frac{3d}{2}}.
\end{aligned} \tag{49}$$

For this case, since the dependance of Y'_G on T_R is different from that of Ω , we get a more complicated expression for δ' , depending explicitly on the number of extra dimensions and C :

$$\delta' < \frac{n_\gamma \xi_B}{B_{\text{EM/Had}} \beta(d) C s_0 m_{\text{KK}}} \left[\frac{\Omega_{B^1} \rho_c - s_0 m_{\text{KK}} d Y_\infty}{\alpha(d) s_0 C m_{\text{KK}}^2} \right]^{-\frac{2+3d}{4+3d}} \tag{50}$$

This is plotted in Fig. 8. As anticipated, the bounds on δ' are much weaker than on δm_{KK} . However, even though the constraint is much weaker now than before, only small mass differences, smaller than about 10 GeV, are allowed in most of the parameter space.

6.6 Diffuse Photon Flux Constraints on the $G^1 - B^1$ Mass Difference

Since the G^1 decays late to the B^1 we have to consider its effect on the diffuse photon flux. As long as the G^1 decays after matter domination, it can have an effect on the diffuse photon flux. Since the observed flux is smooth to a high degree, we can derive a constraint on the mass difference Δ_1 between G^1 and B^1 by requiring that Eq. (29) be less than Eq. (31). Using this inequality, we are led to:

$$\Delta_1 > \left(2.48 \times 10^{-3} \left(\left[\frac{T_R}{m_{\text{KK}}} \right]^{3/2} - 1 \right) \left[\frac{m_{\text{KK}}}{\text{TeV}} \right] \right)^{1/2} \text{ GeV}, \quad (51)$$

where T_R is given by Eq. (40). This is plotted in Fig. 9. We see again that as m_{KK} approaches the value consistent with the dark matter density without gravitons, the constraint on Δ_1 becomes very weak. At these masses, even if the G^1 were decaying right now, their density is so small that the decays are basically invisible and don't affect the photon spectrum.

6.7 Comparison of Constraints

Comparing the constraints on the mass difference between B^1 and G^1 , plotted in Fig. 10, we see that there is a region of parameter space where both conditions are satisfied. The allowed region increases for larger values of C , and for $C = 1$, extends up to values of order 600 GeV, which is about the value of the bound placed by precision electroweak tests for a light Higgs boson. The range of allowed values of Δ_1 shrinks for decreasing values of $m_{\text{KK}}/m_{\text{WG}}$. For instance, in the case represented in Fig. 10 for $C = 1$, values of $m_{\text{KK}} \simeq 0.8$ TeV may be obtained for a range of values of $\Delta_1 \sim \mathcal{O}(1)$ GeV, while values as low as $m_{\text{KK}} \sim 0.6$ TeV are only allowed for $\Delta_1 \sim 0.6$ GeV. Interestingly enough the allowed values of m_{KK} agree with the ones consistent with the observed dark matter relic density for $T_R \lesssim 40 m_{\text{KK}}$ depicted in Fig. 2.

The effects on the allowed values of Δ_1 as m_{WG} changes are illustrated in Figs. 11 and 12. As shown in these figures, the qualitative behavior for the different m_{WG} is the same as the one found in Fig. 10.

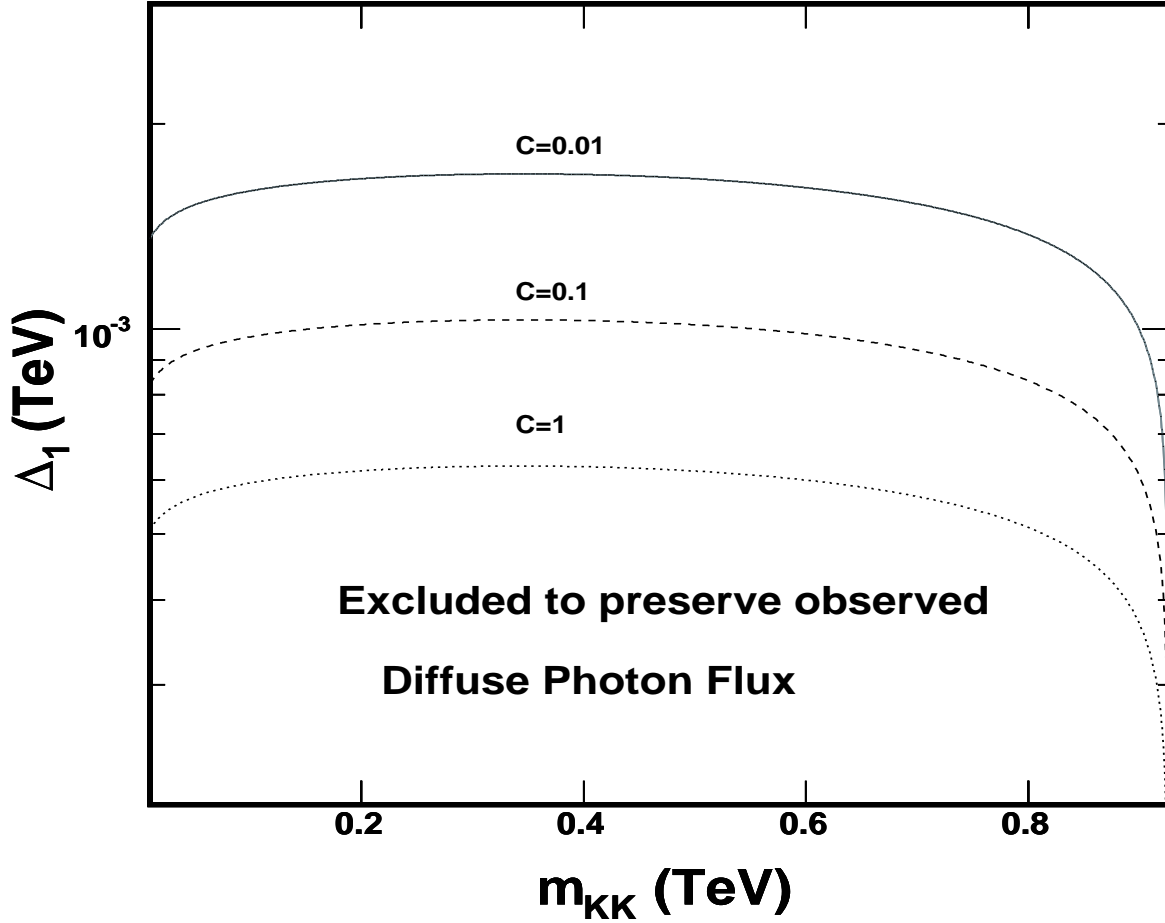


Figure 9: Constraints on the value of the mass difference between G^1 and the LKP, Δ_1 , assuming $\Omega_{\text{DM}} = 0.23$ for $D = 5$, $C = 1, 0.1$ and 0.01 . We have ignored possible coannihilation and second KK level effects.

6.8 One Loop Corrections to the KK Masses

We want to compare the bounds obtained on Δ_1 due to BBN and the diffuse photon flux found in the previous section, with the one-loop corrections induced in the B^1 mass, assuming that $m_{G^1} = 1/R$. Radiative corrections induced by boundary terms at the orbifold fixed points affect the spectrum of the standard KK particles. Since radiative corrections are divergent they may be regularized by counterterms localized at these boundaries. The possibility of including localized counterterms also implies that one could have started with different values of the localized boundary terms than the ones assumed in the minimal scenario, and this would lead to modifications of the spectrum different from the one discussed below [32]. We include, however, a discussion of this minimal scenario in order to show that, interestingly enough, the magnitude of the one-loop induced corrections is indeed of the order of the one

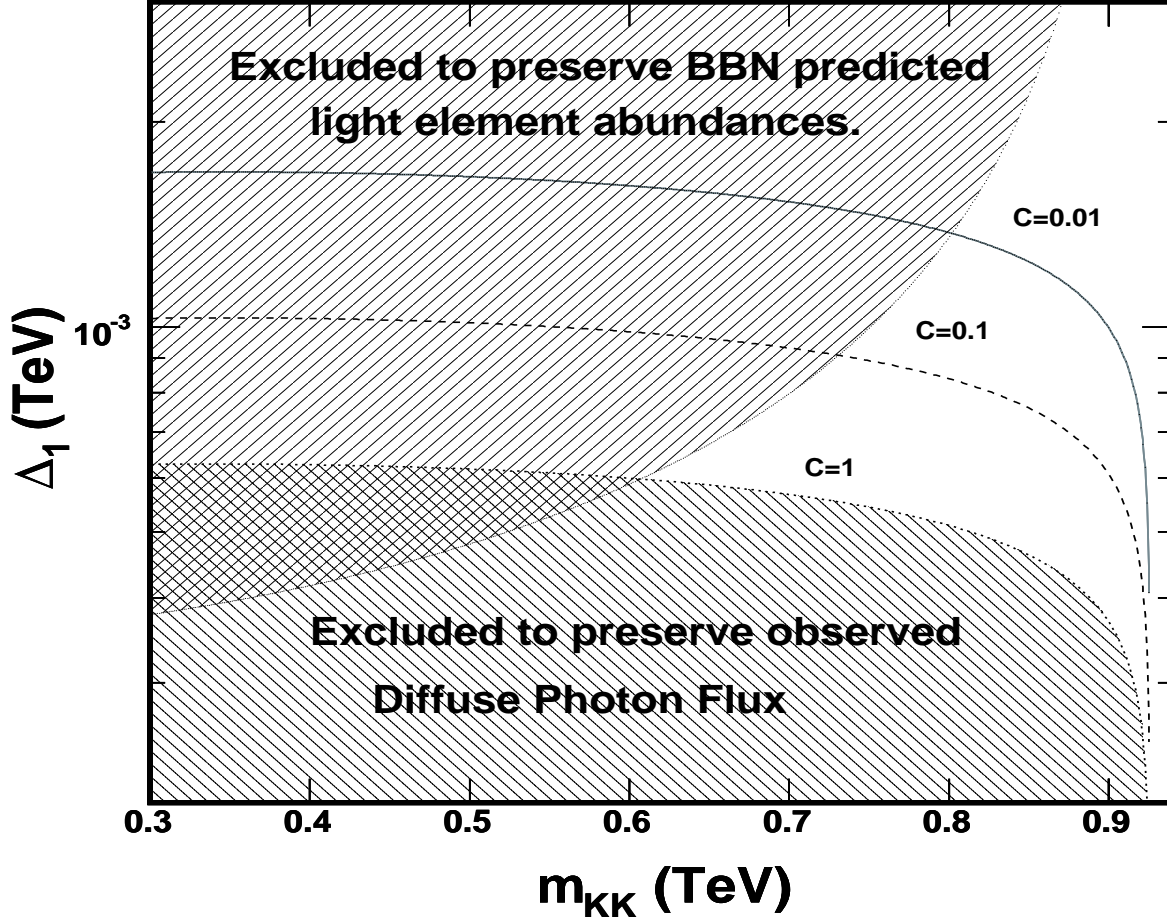


Figure 10: Constraints on the value of the mass difference between G^1 and the LKP, Δ_1 , assuming $\Omega_{\text{DM}} = 0.23$ for $D = 5$, $C = 1, 0.1$ and 0.01 . We have ignored possible coannihilation and second KK level effects.

necessary to satisfy the BBN and diffuse gamma ray bounds.

In order to compute the LKP mass, apart from the one-loop corrections, one must also take into account the $g_i^2 v^2/4$ correction to the gauge boson mass matrix due to the vev of the Higgs field [19]. In the B^n, W_3^n basis:

$$\begin{pmatrix} \frac{n^2}{R^2} + \delta(m_{B^n}^2) + \frac{1}{4} g_1^2 v^2 & \frac{1}{4} g_1 g_2 v^2 \\ \frac{1}{4} g_1 g_2 v^2 & \frac{n^2}{R^2} + \delta(m_{W_3^n}^2) + \frac{1}{4} g_2^2 v^2 \end{pmatrix} \quad (52)$$

Since the mixing is very small compared to the mass difference between the B^n and the W_3^n induced at the one-loop level, the neutral gauge bosons approximately

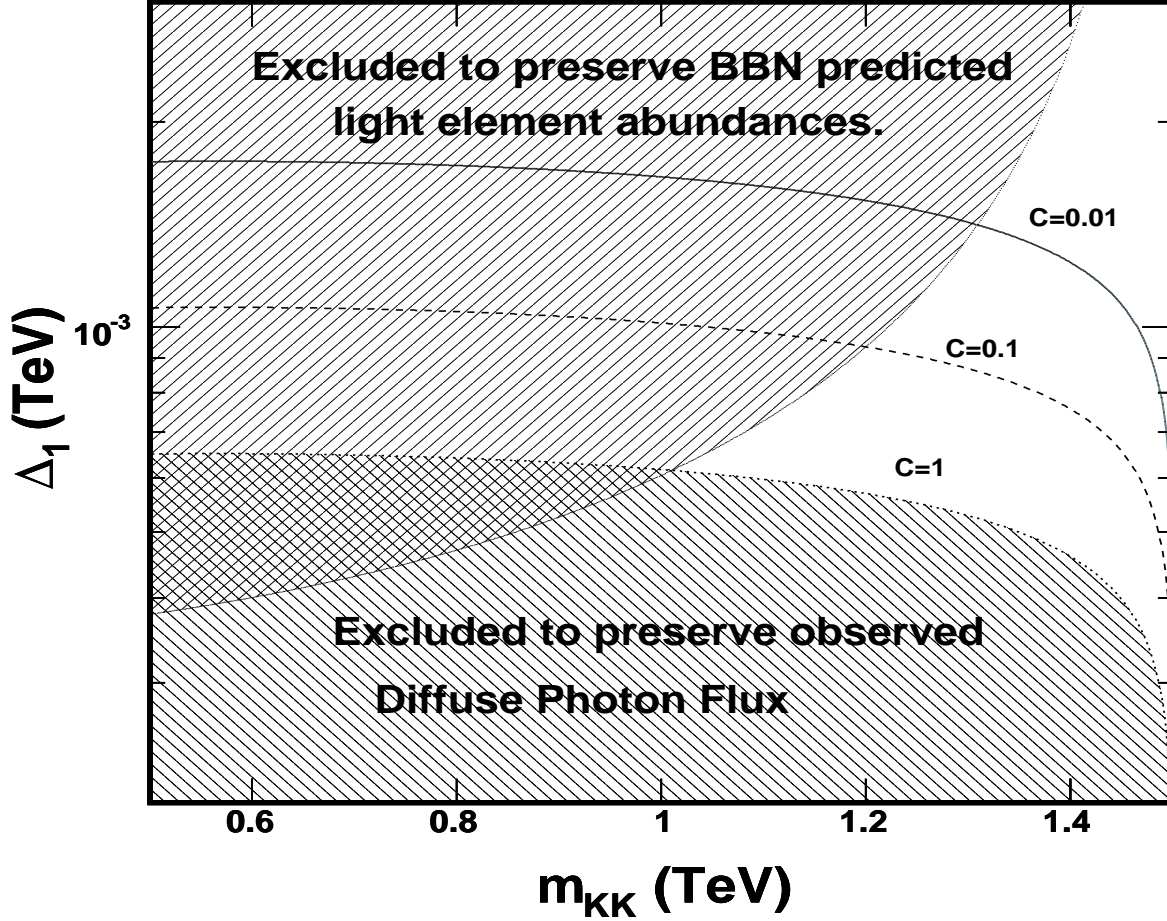


Figure 11: Same as Fig. 10, but for a value of $m_{WG} = 1.5$ TeV.

become pure B^n and W_3^n . Therefore, the mass correction to B^1 is very well approximated by:

$$\delta(m_{B^1}^2) \simeq - \left[\frac{39}{2} \frac{\alpha_1 \zeta(3)}{4\pi^3} + \frac{1}{6} \frac{\alpha_1}{4\pi} \ln \frac{\Lambda^2}{\mu^2} \right] \left(\frac{1}{R} \right)^2 + \frac{g_1^2 v^2}{4}, \quad D=5 \quad (53)$$

This correction to B^1 becomes positive for masses below about 800 GeV, and the absolute value is plotted in Fig. 13. Therefore, as noted in [10], below this mass, assuming only one-loop corrections, the graviton is the LKP. This case has been extensively studied and the constraints are derived in Ref. [22]. The B^1 s, with a density comparable to $\Omega \sim 0.23$, would be decaying late to G^1 and based on an analysis similar to the one performed in Section 4, one concludes that, apart from the finely tuned case in which the mass difference approximately vanishes, small mass differences between the B^1 and the G^1 would lead to a large impact on the diffuse photon flux. Therefore, unless some evidence is seen in the diffuse photon

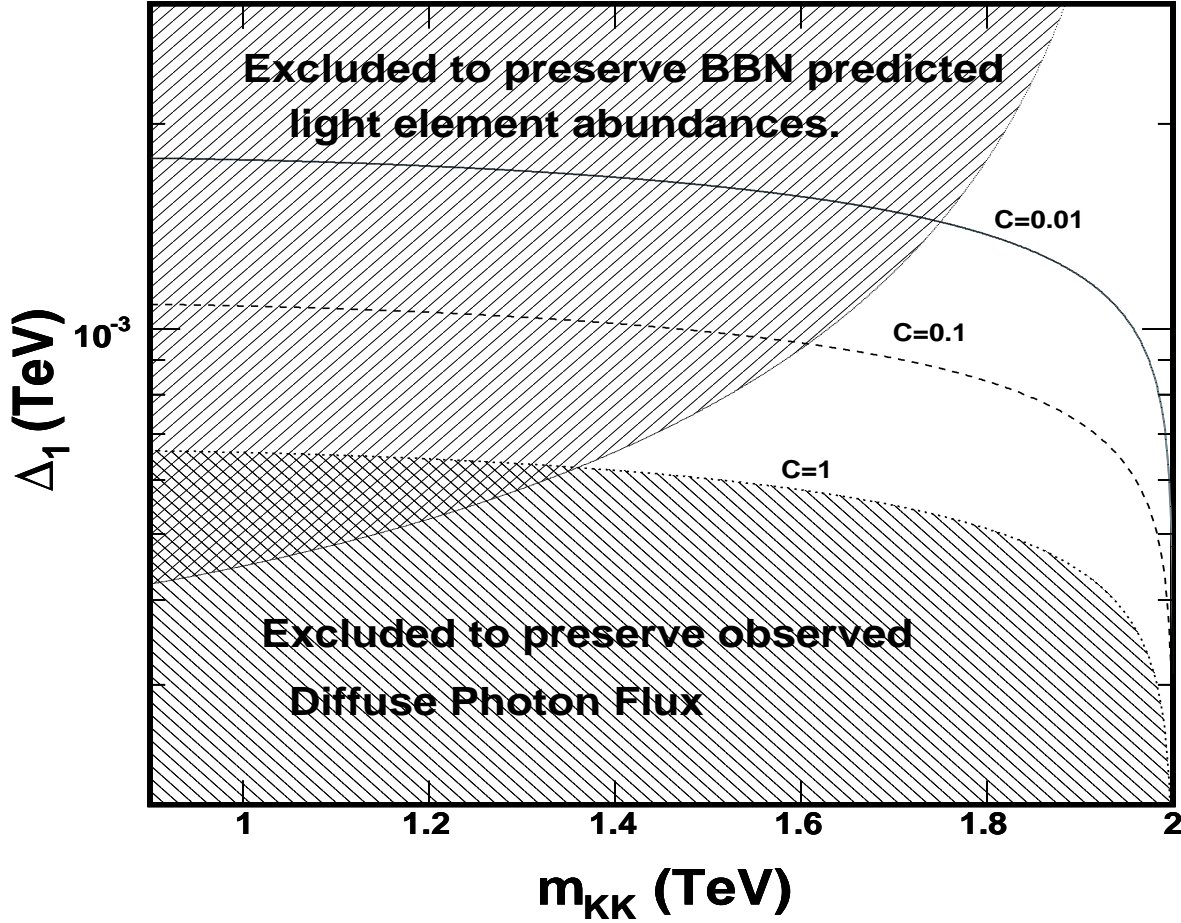


Figure 12: Same as Fig. 10, but for a value of $m_{\text{WG}} = 2$ TeV.

flux for new physics for values of $E_\gamma \sim \mathcal{O}(1)$ MeV (see Fig. 1), this minimal scenario would be ruled out for $m_{\text{KK}} < 800$ GeV³.

We see that in the allowed region demarcated in Figs. 10, 11 and 12 the values of Δ_1 are, as emphasized before, of the same order of magnitude as the range predicted by the one loop corrections shown in Fig. 13. The precise quantitative constraints on the possible values of $m_{\text{KK}}/m_{\text{WG}}$ depend on m_{WG} . While for $m_{\text{WG}} \simeq 1, 2$ TeV, only corrections of the order of ten percent would be allowed, for $m_{\text{WG}} \simeq 1.5$ TeV, the one-loop corrections are consistent with those necessary to satisfy both the BBN and diffuse photon flux constraints⁴.

In evaluating these constraints we have to stress again that we have used a very

³Please see Ref. [34] for a possible solution to this problem, by the introduction of Dirac neutrinos.

⁴In Ref. [10] it was argued that, within this minimal framework, values of $m_{\text{WG}} > 1.4$ TeV would be disfavored since a charged Higgs would become the LKP.

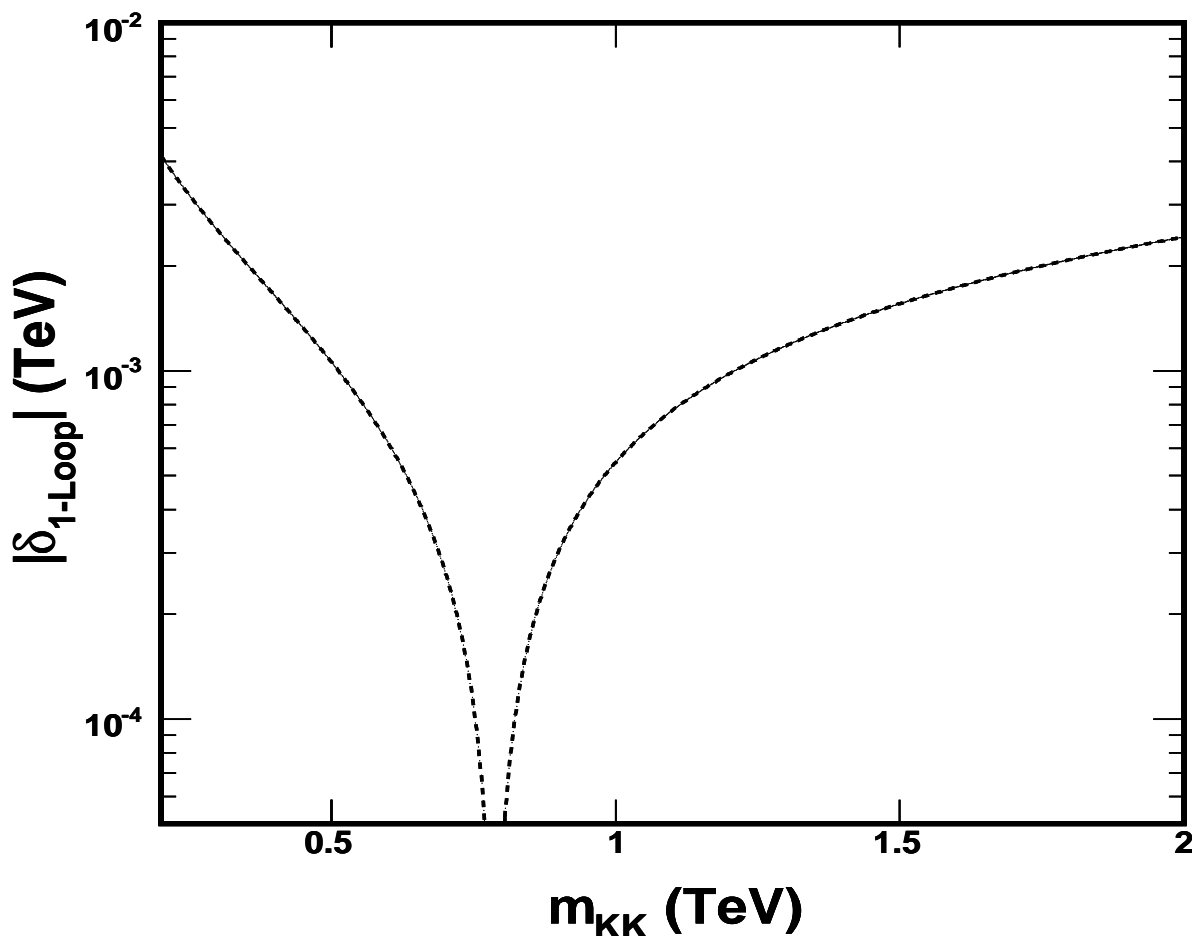


Figure 13: One loop corrections to the B^1 mass as a function of m_{KK} .

conservative estimate for the hadronic branching ratio of $B_H = 1$. The actual energy released into hadrons is approximately proportional to B_H and would be somewhat lower since the KK quarks are much heavier than the KK right handed leptons. Additionally there are large errors in the detection of the diffuse photon flux. A proper computation of the hadronic branching ratio of the decay of gravitons, as well as a more accurate spectrum for the diffuse photon flux, would be necessary in order to determine the compatibility of this minimal scenario with the energy release constraints.

6.9 Determination of the Reheating Temperature

Let us finish this section by commenting on the possible experimental probes of this scenario. Due to their small couplings to matter, provided G^1 is not the LKP, the KK gravitons will not be produced at laboratory experiments. Therefore, their

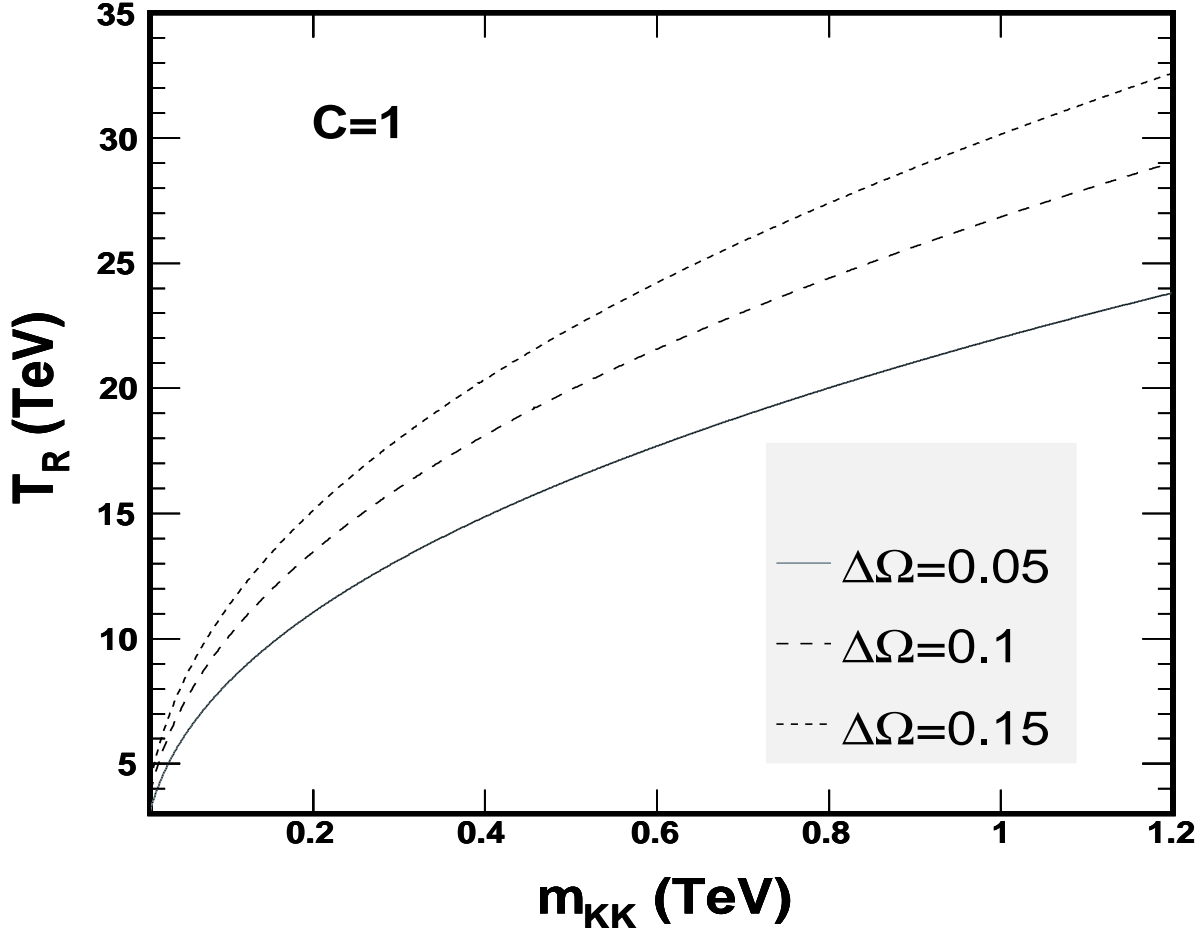


Figure 14: The reheating temperature, T_R , required to make up the deficit dark matter density by KK gravitons as dictated by Eq. (54).

presence may only be probed by indirect effects, like their impact on cosmology as we have discussed in this article. In order to be able to evaluate these effects, one would have to find conclusive evidence of UED at, for instance, collider experiments and, in addition, measure the properties of the relevant first and second KK modes that contribute to the B^1 annihilation cross section. Then, under the assumption that no other exotic particle contributes to the dark matter density one could estimate the relic density associated with the LKP for the specific value of m_{KK} measured. If the obtained relic density disagrees with the experimentally measured one, then one would get information about the possible KK graviton contribution.

Knowledge of the graviton contribution and the KK mass m_{KK} will, in turn, allow us to determine the reheating temperature. By analogy with Eq. (40), the

reheating temperature for one extra dimension would be given by,

$$T_R = m_{\text{KK}} \left(\frac{\Delta\Omega \rho_c}{\alpha(1) C s_0 m_{\text{KK}}^2} \right)^{2/7}, \quad (54)$$

where $\Delta\Omega$ is the difference between the measured value of Ω and the theoretically estimated one from the measured value of m_{KK} and the corresponding annihilation cross section. This is plotted for $C = 1$ in Fig. 14 for several different values of $\Delta\Omega$ for reference. Even including the possibility of exotic particles contributing to the dark matter density, Eq. (54) gives an upper limit on the reheating temperature.

7 Conclusions

In this article, we analyzed the effects of including the KK graviton tower on the determination of the relic density associated with the lightest KK particle in the scenario of Universal Extra Dimensions. Gravitons may be copiously produced in the early universe and their subsequent decay into the LKP may lead to a modification of the observed LKP relic density. Graviton production is governed by a parameter $C \sim \mathcal{O}(1)$ and by the reheating temperature, which is bounded from above by the requirement of maintaining the perturbative consistency of the theory, $T_R < 40m_{\text{KK}}$ ($T_R < 10m_{\text{KK}}$) for $D = 5$ ($D = 6$). In the case that Universal Extra Dimensions are observed in laboratory experiments, we show that an upper limit on the reheating temperature can be deduced from the requirement that only the LKP contributes to the observed dark matter density.

Throughout this work we have assumed KK parity conservation, leading to the stability of the LKP particle. We found that including the graviton effectively lowers the lightest KK particle mass consistent with the observed dark matter relic density from values of about 0.92 TeV to values as low as $m_{\text{KK}} \sim 0.58$ TeV for $C = 1$, $D = 5$ and $T_R < 40 m_{\text{KK}}$. Additionally, including effects which change the LKP density (coannihilation, second KK-level mode resonant contributions, etc.), we show that the graviton tower has a large impact on the predicted mass of the LKP with increasing mass. It should be stressed here that these results are independent of which KK particle is the LKP (or the NLKP).

Additionally, there are bounds on the mass difference of the LKP with the graviton KK modes induced by the requirement that the energy released in the graviton decay does not lead to a disturbance of the light element abundance or the diffuse photon flux. Under the assumption that the graviton spectrum is $m_{G^n} \sim n/R$, we have obtained a bound on the mass difference of G^1 and the LKP (B^1) mass, that is consistent with the minimal one-loop corrections obtained in Ref. [19] for a large range of values of m_{KK} .

Acknowledgements: We would like to thank Jonathan Feng, Csaba Balazs and Tim Tait for useful discussions and comments. Work at ANL is supported in part by the US DOE, Div. of HEP, Contract W-31-109-ENG-38. This work was also supported in part by the U.S. Department of Energy through Grant No. DE-FG02-90ER40560.

References

- [1] I. Antoniadis, Phys. Lett. B **246**, 377 (1990).
- [2] T. Appelquist, H. C. Cheng and B. A. Dobrescu, Phys. Rev. D **64**, 035002 (2001) [arXiv:hep-ph/0012100].
- [3] T. Appelquist and H. U. Yee, Phys. Rev. D **67**, 055002 (2003) [arXiv:hep-ph/0211023].
- [4] G. Servant and T. M. P. Tait, Nucl. Phys. B **650**, 391 (2003) [arXiv:hep-ph/0206071].
- [5] K. Griest and D. Seckel, Phys. Rev. D **43**, 3191 (1991).
- [6] M. Kakizaki, S. Matsumoto, Y. Sato and M. Senami, Phys. Rev. D **71**, 123522 (2005) [arXiv:hep-ph/0502059].
- [7] M. Kakizaki, S. Matsumoto, Y. Sato and M. Senami, Nucl. Phys. B **735**, 84 (2006) [arXiv:hep-ph/0508283].
- [8] K. Kong and K. T. Matchev, JHEP **0601**, 038 (2006) [arXiv:hep-ph/0509119].
- [9] F. Burnell and G. D. Kribs, Phys. Rev. D **73**, 015001 (2006) [arXiv:hep-ph/0509118].
- [10] M. Kakizaki, S. Matsumoto and M. Senami, Phys. Rev. D **74**, 023504 (2006) [arXiv:hep-ph/0605280].
- [11] E. W. Kolb, G. Servant and T. M. P. Tait, JCAP **0307**, 008 (2003) [arXiv:hep-ph/0306159].
- [12] J. L. Feng, A. Rajaraman and F. Takayama, Phys. Rev. D **68**, 085018 (2003) [arXiv:hep-ph/0307375].
- [13] J. R. Ellis, K. A. Olive and E. Vangioni, Phys. Lett. B **619**, 30 (2005) [arXiv:astro-ph/0503023].
- [14] M. Kawasaki, K. Kohri and T. Moroi, Phys. Rev. D **71**, 083502 (2005) [arXiv:astro-ph/0408426].

- [15] R. H. Cyburt, J. R. Ellis, B. D. Fields and K. A. Olive, Phys. Rev. D **67**, 103521 (2003) [arXiv:astro-ph/0211258].
- [16] P. Sreekumar, F. W. Stecker and S. C. Kappadath, AIP Conf. Proc. **510**, 459 (2004) [arXiv:astro-ph/9709258].
- [17] M. Kawasaki, K. Kohri and T. Moroi, Phys. Lett. B **625**, 7 (2005) [arXiv:astro-ph/0402490].
- [18] K. Jedamzik, Phys. Rev. D **70**, 063524 (2004) [arXiv:astro-ph/0402344].
- [19] H. C. Cheng, K. T. Matchev and M. Schmaltz, Phys. Rev. D **66**, 036005 (2002) [arXiv:hep-ph/0204342].
- [20] M. Bolz, W. Buchmuller and M. Plumacher, Phys. Lett. B **443**, 209 (1998) [arXiv:hep-ph/9809381].
- [21] M. Bolz, A. Brandenburg and W. Buchmuller, Nucl. Phys. B **606**, 518 (2001) [arXiv:hep-ph/0012052].
- [22] J. L. Feng, A. Rajaraman and F. Takayama, Phys. Rev. Lett. **91**, 011302 (2003) [arXiv:hep-ph/0302215].
- [23] J. L. Feng, A. Rajaraman and F. Takayama, Phys. Rev. D **68**, 063504 (2003) [arXiv:hep-ph/0306024].
- [24] T. Flacke, D. Hooper and J. March-Russell, Phys. Rev. D **73**, 095002 (2006) [Erratum-ibid. D **74**, 019902 (2006)] [arXiv:hep-ph/0509352].
- [25] I. Gogoladze and C. Macesanu, arXiv:hep-ph/0605207.
- [26] R. S. Chivukula, D. A. Dicus, H. J. He and S. Nandi, Phys. Lett. B **562**, 109 (2003) [arXiv:hep-ph/0302263].
- [27] R. S. Chivukula, D. A. Dicus, H. J. He and S. Nandi, arXiv:hep-ph/0402222.
- [28] M. Masip, Phys. Rev. D **62**, 105012 (2000) [arXiv:hep-ph/0007048].
- [29] M. E. Peskin and D. V. Schroeder, “An Introduction to quantum field theory” , Addison Wesley, 1995.
- [30] P. Ramond, “Journeys beyond the standard model” , Perseus Books, 1999.
- [31] D. R. T. Jones, Phys. Rev. D **25**, 581 (1982).
- [32] M. Carena, T. M. P. Tait and C. E. M. Wagner, Acta Phys. Polon. B **33**, 2355 (2002) [arXiv:hep-ph/0207056].

- [33] C. Macesanu, A. Mitov and S. Nandi, Phys. Rev. D **68**, 084008 (2003)
[arXiv:hep-ph/0305029].
- [34] S. Matsumoto, J. Sato, M. Senami and M. Yamanaka, arXiv:hep-ph/0607331.
- [35] <http://home.earthlink.net/~djmp/TensorialPage.html>

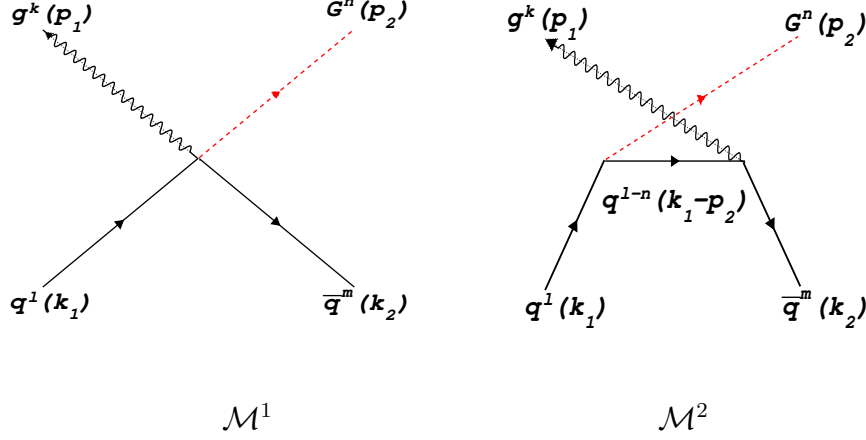


Figure A.1: Feynman Diagrams contributing to $q^l + \bar{q}^m \rightarrow g^k + G^n$. The corresponding amplitudes are given in (A.5) and (A.6).

APPENDIX

A Graviton Production Cross-Section

We will calculate explicitly the graviton production cross-section for $q^l(k_1) + \bar{q}^m(k_2) \rightarrow g^k(p_1) + G^n(p_2)$. The feynman rules we will need are [12, 33]:

$$q^l(k_1) \rightarrow q^m(k_2) + G^n(p_2) :$$

$$\begin{aligned}
Y^{\mu\nu} &= \frac{i}{4M_4} \left(-\eta^{\mu\nu} (k_1 + k_2 - m_{m\pm l}) + \frac{1}{2} \gamma^\mu (k_1 + k_2)^\nu + \frac{1}{2} \gamma^\nu (k_1 + k_2)^\mu \right) \\
&\times [\delta_{n,|l-m|} - \gamma^5 \delta_{n,l+m}]
\end{aligned} \tag{A.1}$$

$$g_\alpha^l(k_1) \rightarrow g_\beta^m(k_2) + G_{\mu\nu}^n :$$

$$\begin{aligned}
X^{\mu\nu\alpha\beta} &= -\frac{i}{2M_4} \left[(-m_l m_m + k_1 \cdot k_2) \left(-\eta^{\mu\nu} \eta^{\alpha\beta} + \eta^{\mu\alpha} \eta^{\nu\beta} + \eta^{\mu\beta} \eta^{\nu\alpha} \right) + \eta^{\mu\nu} k_1^\beta k_2^\alpha \right. \\
&\quad \left. - \left(\eta^{\mu\beta} k_1^\nu k_2^\alpha + \eta^{\mu\alpha} k_1^\beta k_2^\nu - \eta^{\alpha\beta} k_1^\mu k_2^\nu + (\nu \leftrightarrow \mu) \right) \right] \delta_{n,|l-m|}
\end{aligned} \tag{A.2}$$

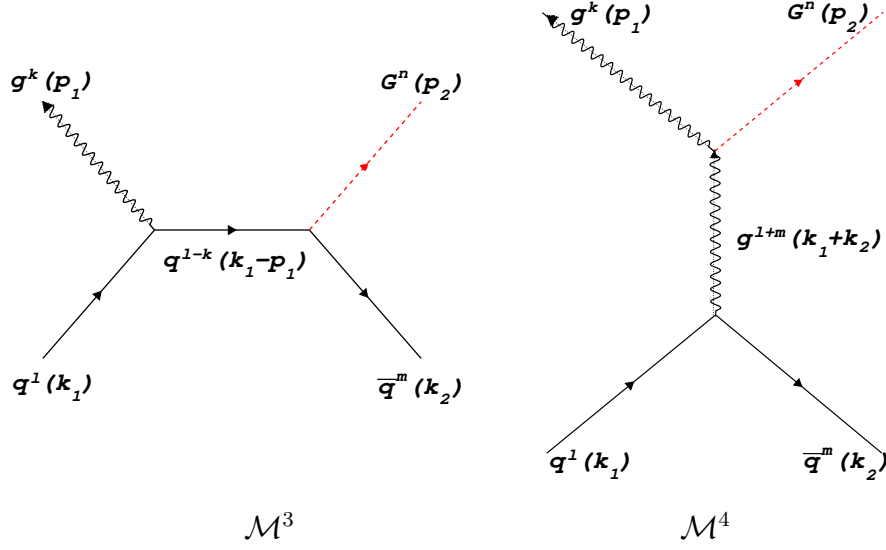


Figure A.2: Feynman Diagrams contributing to $q^l + \bar{q}^m \rightarrow g^k + G^n$. The corresponding amplitudes are given in (A.7) and (A.8).

$$q + \bar{q} \rightarrow g :$$

$$Z^\mu = ig\gamma^\mu t^a \quad (\text{A.3})$$

$$q^l + \bar{q}^m \rightarrow g^{k\rho} + G^{m\mu\nu} :$$

$$A^{\mu\nu\rho} = \frac{igt^a}{4M_4} (-2\eta^{\mu\nu}\gamma^\rho + \eta^{\mu\rho}\gamma^\nu + \eta^{\nu\rho}\gamma^\mu) \gamma^5 \delta_{l+m,k+n} \quad (\text{A.4})$$

Four diagrams contribute to this process (Fig. A.1, A.2). The amplitudes are given by:

$$\mathcal{M}^1 : \quad \frac{igt^a}{2M_4} \bar{v}(k_2) \left[\gamma^\nu \epsilon^{*\mu} e_{\mu\nu}^* - \gamma^\nu \epsilon_\nu^* e_\mu^{*\mu} \right] \gamma^5 u(k_1) \quad (\text{A.5})$$

$$\mathcal{M}^2 : \quad -\frac{igt^a}{4M_4} \bar{v}(k_2) \gamma^\rho \frac{k_1 - \not{p}_2 + m_{l-n}}{2(k_1 \cdot p_2 - m_l m_n)} (\eta^{\mu\nu} (\not{p}_2 - m_n) + \gamma^\mu k_1^\nu + \gamma^\nu k_1^\mu) u(k_1) \epsilon_\rho^* e_{\mu\nu}^* \quad (\text{A.6})$$

$$\mathcal{M}^3 : \frac{igt^a}{4M_4} \bar{\nu}(k_2) \frac{\eta^{\mu\nu}(\not{k}_1 - \not{p}_1 + m_{l-k}) - \gamma^\mu k_2^\nu - \gamma^\nu k_2^\mu}{2(k_1 \cdot p_1 - m_l m_k)} \gamma^5 (2k_1^\rho - (\not{p}_1 + m_k)\gamma^\rho) u(k_1) \epsilon_\rho^* e_{\mu\nu}^* \quad (\text{A.7})$$

$$\mathcal{M}^4 : \frac{igt^a}{2M_4} \frac{\bar{\nu}(k_2)}{(k_1 + k_2)^2 - m_{l+m}^2} [(m_k m_{k-l-m} + p_1 \cdot p_2) (\gamma^\rho \eta^{\mu\nu} - \gamma^\mu \eta^{\nu\rho} - \gamma^\nu \eta^{\mu\rho}) - (\eta^{\mu\nu} p_2^\rho - \eta^{\mu\rho} p_1^\nu - \eta^{\nu\rho} p_1^\mu) \not{p}_1 - 2\gamma^\rho p_1^\mu p_1^\nu + (\gamma^\mu p_1^\nu + \gamma^\nu p_1^\mu) p_2^\rho] u(k_1) \epsilon_\rho^* e_{\mu\nu}^* \quad (\text{A.8})$$

In the center-of-mass frame, the cross-section is given by [29]:

$$\left(\frac{d\sigma}{d\Omega} \right)_{CM} = \frac{1}{2E_1 2E_2 |\nu_1 - \nu_2|} \frac{|\mathbf{p}_2|}{(2\pi)^2 4E_{CM}} |\mathcal{M}(k_1, k_2 \rightarrow p_1, p_2)|^2. \quad (\text{A.9})$$

Here, E_1, E_2 and ν_1, ν_2 label the initial particle energies and velocities, and \mathbf{p}_2 is the three-momentum of the graviton. Since we are interested in the relativistic limit, we can use the more general form for all four particles with $m = 0$:

$$\left(\frac{d\sigma}{d\Omega} \right)_{CM} = \frac{|\mathcal{M}|^2}{32\pi^2 |\nu_1 - \nu_2| E_{CM}^2}. \quad (\text{A.10})$$

Averaging over initial spins and colors and summing over final polarizations, $|\mathcal{M}|^2$ was calculated using the **Tensorial 3.0** package for *Mathematica* [35]. The cross-section is then given by:

$$\langle \sigma \nu \rangle = \frac{\alpha_3}{4\pi M_4^2} d(G) C(r) \pi \frac{1184 + 105\pi}{1296}. \quad (\text{A.11})$$

The fraction of strongly interacting degrees of freedom per KK level is computed by counting the different allowed interactions. Four strong interactions can produce gravitons:

$$\begin{aligned} q + \bar{q} &\rightarrow g + G \\ g + q &\rightarrow q + G \\ g + \bar{q} &\rightarrow \bar{q} + G \\ g + g &\rightarrow g + G \end{aligned}$$

There are $2 \times 3 \times 24$ degrees of freedom for the quarks and 3×8 for the gluons. The fraction can then be calculated:

$$p_{s^2} = 24 \left[\left(\frac{7}{8} \right)^2 \left(\frac{6}{197.5} \right)^2 + 2 \left(\frac{7}{8} \right) \left(\frac{24}{197.5} \right) \left(\frac{6}{197.5} \right) \right] + \left(\frac{24}{197.5} \right)^2 \sim 0.19. \quad (\text{A.12})$$

Assuming that all the other graviton production processes have a cross-section similar to (A.11), C used to parameterize the graviton production cross-section is given by:

$$\begin{aligned} C &= p_{s^2} d(G) C(r) \pi \frac{1184 + 105\pi}{1296} = 2.79, \\ &\sim \mathcal{O}(1). \end{aligned} \quad (\text{A.13})$$

B Decay Lifetimes

The graviton polarization sum is given by [12]:

$$\begin{aligned} \sum_s e_{\mu\nu}^s e_{\rho\sigma}^{s*} &= B_{\mu\nu\rho\sigma} \\ B_{\mu\nu\rho\sigma}(k) &= 2 \left(\eta_{\mu\rho} - \frac{k_\mu k_\rho}{m_n^2} \right) \left(\eta_{\nu\sigma} - \frac{k_\nu k_\sigma}{m_n^2} \right) + 2 \left(\eta_{\mu\sigma} - \frac{k_\mu k_\sigma}{m_n^2} \right) \left(\eta_{\nu\rho} - \frac{k_\nu k_\rho}{m_n^2} \right) \\ &\quad - \frac{4}{3} \left(\eta_{\mu\nu} - \frac{k_\mu k_\nu}{m_n^2} \right) \left(\eta_{\rho\sigma} - \frac{k_\rho k_\sigma}{m_n^2} \right) \end{aligned} \quad (\text{B.1})$$

The decay width of $G^n(p) \rightarrow f^l(k_1) + \bar{f}^m(k_2)$ summed over final and averaged over initial polarizations is:

$$\begin{aligned} \Gamma(G^n \rightarrow f^l + \bar{f}^m) &= \frac{|\mathbf{k}_1|}{8\pi m_n^2} \frac{1}{5} \sum_{s,s'} \bar{u}^s(k_2) Y^{\mu\nu} \nu^{s'}(k_1) \bar{\nu}^{s'}(k_1) Y^{*\alpha\beta} u^s(k_2) B_{\mu\nu\alpha\beta} \\ &= \frac{1}{160\pi} \frac{m_n^3}{M_4^2} \left[1 - \frac{(m_l - m_m)^2}{m_n^2} \right]^{3/2} \left[1 - \frac{(m_l + m_m)^2}{m_n^2} \right]^{5/2} \\ &\quad \times \left[1 + \frac{2(m_l - m_m)^2}{m_n^2} \right]. \end{aligned} \quad (\text{B.2})$$

This is suppressed for $l \neq m$. Therefore assuming that the main decay is into $l = m = n/2$:

$$\Gamma(G^n \rightarrow f^{m=n/2} + \bar{f}^{m=n/2}) = \frac{1}{160\pi} \frac{m_n^3}{M_4^2} \left[1 - \frac{4m_m^2}{m_n^2} \right]^{5/2}. \quad (\text{B.3})$$

The decay width of $G^n(p) \rightarrow B^l(k_1) + B^m(k_2)$ summed over final and averaged over initial polarizations is given by:

$$\Gamma(G^n \rightarrow B^l + B^m) = \frac{|\mathbf{k}_1|}{8\pi m_n^2} \frac{1}{5} X^{\mu\nu\alpha\beta} X^{*\rho\sigma\lambda\kappa} \left(\eta_{\alpha\lambda} - \frac{k_{1\alpha} k_{1\lambda}}{m_m^2} \right) \left(\eta_{\beta\kappa} - \frac{k_{2\beta} k_{2\kappa}}{m_l^2} \right) B_{\mu\nu\rho\sigma}$$

$$\begin{aligned}
&= \frac{\cos^2 \theta_W}{80\pi} \frac{m_n^3}{M_4^2} \left[1 - \frac{(m_l - m_m)^2}{m_n^2} \right]^{5/2} \left[1 - \frac{(m_l + m_m)^2}{m_n^2} \right]^{1/2} \\
&\quad \times \left[\frac{13}{6} + \frac{7}{3} \frac{(m_l + m_m)^2}{m_n^2} + \frac{1}{2} \frac{(m_l + m_m)^4}{m_n^4} \right].
\end{aligned} \tag{B.4}$$

We see again that the decay into KK modes other than $n/2$ is suppressed. Therefore for all $n > 1$, assuming now that the main decay is in fact into $B^{n/2} + B^{n/2}$ with an extra factor of 1/2 for identical particles in the final state:

$$\Gamma(G^n \rightarrow 2B^{m=n/2}) = \frac{\cos^2 \theta_W}{80\pi} \frac{m_n^3}{M_4^2} \left[1 - \frac{4m_m^2}{m_n^2} \right]^{1/2} \left[\frac{13}{12} + \frac{14}{3} \frac{m_m^2}{m_n^2} + 4 \frac{m_m^4}{m_n^4} \right], \tag{B.5}$$

with $\Delta_n \equiv m_n - 2m_m \sim m_{G^n} - m_{B^n} \ll m_n$:

$$\Gamma \sim \frac{\sqrt{2} \cos^2 \theta_W}{32\pi} \frac{m_n^3}{M_4^2} \sqrt{\frac{\Delta_n}{m_n}}. \tag{B.6}$$

For any n decay into a KK gauge boson and a photon:

$$\Gamma(G^n \rightarrow B^n + \gamma) = \frac{\cos^2 \theta_W}{30\pi} \frac{\Delta_n^3}{M_4^2} \left[6 + 3 \frac{m_{B^n}^2}{m_{G^n}^2} + \frac{m_{B^n}^4}{m_{G^n}^4} \right]. \tag{B.7}$$